inoculated with mock-transduced cells, but failed to do so when HDAC1-transduced cells were inoculated. We compared the tumor volume between vehicle-control and bortezomib-treated groups on day 21. As shown in Figure 6D and E, the tumor volume of mock-transduced cells was significantly lower in the bortezomib-treated group than in the vehicle-control group. In contrast, there was no difference in the tumor volume of HDAC1-transduced cells between groups. These results suggest that HDAC1 overexpression confers bortezomib resistance to MM cells in vivo. To confirm the role of HDAC1 in bortezomib resistance, we examined the effects of an HDAC inhibitor on the sensitivity of HDAC1-transduced cells to bortezomib. The addition of romidepsin successfully regressed bortezomib-resistant tumor after 12 days (Figure 6C), and the tumor size was significantly smaller than that of the bortezomib-treated group at 21 days (Figure 6D-E). These results strongly suggest that HDACs are critical targets of bortezomib in vivo.

Discussion

In this study, we have clearly demonstrated that HDACs play a critical role in bortezomib-induced cytotoxicity against MM. The expression of class I HDACs was down-regulated by bortezomib at a transcriptional level via caspase-8–dependent degradation of Sp1 protein, the most potent transactivator of HDACs. As a result, HDAC activities were reduced in MM cells, leading to apoptotic cell death. Because Sp1 is a broadly acting transcription factor, many other target genes should be repressed by Sp1 down-regulation in bortezomib-treated MM cells. Using loss-of-function and gain-of-function analyses, however, we confirmed that sensitivity to bortezomib depends on the levels of HDAC1 expression in MM cells both in vitro and in vivo. This implies that HDACs are critical targets of Sp1 for bortezomib-induced cytotoxicity, although the involvement of other molecules cannot be ruled out. Taken together, our present findings may address the emerging question about the targets of bortezomib,[24] add a novel and critical determinant in a list of effector molecules of bortezomib,[42] and thus provide a novel rationale for the use of proteasome inhibitors in the treatment of patients with MM.

In support of our findings, recent evidence has suggested a close link between proteasome inhibitors and HDACs. Catley et al[43] reported that a hydroxamic acid–derivative NVP-LAQ824, referred to an HDAC inhibitor, affects proteasome activities in MM cells. This compound has a unique ability in overcoming cell adhesion–mediated drug resistance (CAM-DR) of MM cells. Recently, we have shown that VLA-4 is a key molecule of CAM-DR in MM cells, and bortezomib can overcome CAM-DR via the down-regulation of VLA-4 expression.[30] However, our preliminary experiments suggested that HDAC inhibitors, such as romidepsin and valproic acid, did not down-regulate VLA-4 expression but reversed CAM-DR in MM cells (data not shown). The characteristics of NVP-LAQ824 may not be like other HDAC inhibitors but rather resemble bortezomib; therefore, it is possible that NVP-LAQ824 inhibits HDAC activity via the down-regulation of HDAC expression. In addition, Miller et al[44] reported that a novel proteasome inhibitor NPI-0052 induced caspase-8–dependent histone acetylation in leukemia cells. They demonstrated that ubiquitinated histones did not accumulate in response to NPI-0052, indicating that histone hyperacetylation is not solely due to the accumulation of acetylated histones. It is likely that NPI-0052 induces HDAC down-regulation and histone hyperacetylation via the same mechanism as bortezomib, because we have found that bortezomib down-regulated HDAC expression not only in MM cells but also in other hematologic malignant cell lines, such as HL-60 (acute myeloid leukemia), BJA-B (Burkitt lymphoma) and K562 (chronic myelogenous leukemia; data not shown). Therefore, proteasome inhibitors may generally reduce HDAC activity via the down-regulation of HDAC expression in hematologic malignancies. On the other hand, Fotheringham et al[45] reported that HR23b, which shuttles ubiquitinated cargo proteins to the proteasome, is a mediator of HDAC inhibitor–induced cytotoxicity. HDAC inhibitors increased the activity of HR23b and provoked abnormal protein turnover, which resulted in the inhibition of proteasome activities by saturating the proteasome. Furthermore, Mitsiades et al[5,46] screened for target molecules of the HDAC inhibitor SAHA and bortezomib using DNA microarrays. Several molecules (p21, CXCR4, syndecan-1, IGF-1, cyclin B2, cyclin F, and bcl-2) are commonly influenced by SAHA and bortezomib in MM cells. Therefore, HDAC inhibitors and proteasome inhibitors may exert cytotoxicity through overlapping or redundant pathways.

Previous studies showed that the unfolded protein response is a dominant mechanism of bortezomib-induced cytotoxicity.[47] In this study, we have demonstrated that caspase-12 inhibitor, which could inhibit endoplasmic reticulum (ER) stress-induced apoptosis, did not affect bortezomib-induced apoptosis, but caspase-8 inhibitor did (Figure 3G). The caspase-8–mediated pathway is dominant more than the ER stress-mediated pathway in our system. This discrepancy may be attributable to the difference in doses of bortezomib; less than 8nM in our experiments versus more than 10nM in previous studies. Pharmacodynamic studies revealed that serum concentrations of bortezomib decrease to 2 ng/mL (approximately 5nM) or less 4 hours after administration of 1.3 mg/m^2 bortezomib.[48] Therefore, our data may reflect the cellular events in vivo more accurately, and support the notion that the caspase-8/Sp1/HDAC axis is more important than other pathways.

In recent clinical studies, bortezomib proved effective even in the context of heavily pretreated, relapsed and refractory MM; however, primary and secondary bortezomib resistance occurred in more than 50% of patients.[4] The molecular bases of different individual responsiveness to bortezomib remain unclear. Several previous studies have suggested that adaptation or sensitivity to bortezomib depends on the activity of the ubiquitin-proteosome system in MM cells.[49,50] We have demonstrated here that the overexpression of HDAC1 induced bortezomib resistance in vitro and in vivo. The current study is the second to demonstrate that adaptation to bortezomib can indeed be achieved in an MM cell line. Because of the variation of HDAC expression levels, the treatment outcome of bortezomib-treated patients may depend on HDAC activities of MM cells. Importantly, we could overcome the resistance to bortezomib by the combination of the HDAC inhibitor romidepsin in murine xenograft models. HDAC inhibitors, such as romidepsin, SAHA, and tubacin, are promising agents for patients with bortezomib-resistant MM for the following reasons: (1) bortezomib specifically down-regulated the expression of class I HDACs; (2) romidepsin inhibited both class I and II HDAC activities; and (3) HDAC6 knockdown enhanced bortezomib-induced apoptosis (supplemental Figure 10). Therefore, bortezomib is an indispensable agent for MM treatment and combination with other drugs, especially HDAC inhibitors, may be the best treatment strategy for MM treatment. Our findings reinforce the potential clinical utility of combining these 2 agents.

Acknowledgments

We are grateful to Drs Ralph Mazitschek and Stuart L. Schreiber (Broad Institute of Harvard University and Massachusetts Institute of Technology) for providing tubacin and niltubacin. We thank Ms Akiko Yonekura for excellent technical assistance.

This work was supported in part by the High-Tech Research Center Project for Private Universities: Matching Fund Subsidy from MEXT 2002-2006. J.K., T.W., K.N.-H., and K.M. are winners of the Jichi Medical School Young Investigator Award.

Authorship

Contribution: J.K. designed and performed experiments, analyzed data, and drafted the manuscript; T.W., R.S., M.A., K.M., and M.N. performed experiments; T.I. and Y.K. provided clinical samples; K.N.-H. and K.O. provided materials and critically reviewed the manuscript; and Y.F. designed and supervised research and wrote the manuscript.

Conflict-of-interest disclosure: The authors declare no competing financial interests.

Correspondence: Yusuke Furukawa, Division of Stem Cell Regulation, Center for Molecular Medicine, Jichi Medical University, 3311-1 Yakushiji, Shimotsuke, Tochigi 329-0498, Japan; e-mail: furuyu@jichi.ac.jp.

References

1. Kyle RA, Gertz MA, Witzig TE, et al. Review of 1027 patients with newly diagnosed multiple myeloma. *Mayo Clin Proc.* 2003;78(1):21-33.
2. Minucci S, Pelicci PG. Histone deacetylase inhibitors and the promise of epigenetic (and more) treatments for cancer. *Nat Rev Cancer.* 2006; 6(1):38-51.
3. Richardson PG, Mitsiades C, Schlossman R, et al. Bortezomib in the front-line treatment of multiple myeloma. *Expert Rev Anticancer Ther.* 2008; 8(7):1053-1072.
4. Richardson PG, Sonneveld P, Schuster M, et al. Extended follow-up of a phase 3 trial in relapsed multiple myeloma: final time-to-event results of the APEX trial. *Blood.* 2007;110(10): 3557-3560.
5. Mitsiades CS, Mitsiades NS, McMullan CJ, et al. Transcriptional signature of histone deacetylase inhibition in multiple myeloma: biological and clinical implications. *Proc Natl Acad Sci U S A.* 2004;101(2):540-545.
6. Sutheesophon K, Kobayashi Y, Takatoku MA, Ozawa K, Kano Y, Furukawa Y. Histone deacetylase inhibitor depsipeptide (FK228) induces apoptosis in leukemic cells by facilitating mitochondrial translocation of Bax, which is enhanced by the proteasome inhibitor bortezomib. *Acta Haematol.* 2006;115(1-2):78-90.
7. Badros A, Burger AM, Philip S, et al. Phase I study of vorinostat in combination with bortezomib for relapsed and refractory multiple myeloma. *Clin Cancer Res.* 2009;15(16):5250-5257.
8. Herman JG, Baylin SB. Gene silencing in cancer in association with promoter hypermethylation. *N Engl J Med.* 2003;349(21):2042-2054.
9. Marks P, Rifkind RA, Richon VM, Breslow R, Miller T, Kelly WK. Histone deacetylases and cancer: causes and therapies. *Nat Rev Cancer.* 2001;1(3):194-202.
10. Yang X-J, Seto E. The Rpd3/Hda1 family of lysine deacetylases: from bacteria and yeast to mice and men. *Nat Rev Mol Cell Biol.* 2008;9(3):206-218.
11. Lagger G, O'Carroll D, Rembold M, et al. Essential function of histone deacetylase 1 in proliferation control and CDK inhibitor repression. *EMBO J.* 2002;21(11):2672-2681.
12. Lin RJ, Nagy L, Inoue S, et al. Role of the histone deacetylase complex in acute promyelocytic leukemia. *Nature.* 1998;391(6669):811-814.
13. Wang J, Hoshino T, Redner RL, Kajigaya S, Liu JM. ETO, fusion partner in t(8;21) acute myeloid leukemia, represses transcription by interaction with the human N-CoR/mSin3/HDAC1 complex. *Proc Natl Acad Sci U S A.* 1998;95(18):10860-10865.
14. Kobayashi Y, Ohtsuki M, Murakami T, et al. Histone deacetylase inhibitor FK228 suppresses the Ras-MAP kinase signaling pathway by upregulating Rap1 and induces apoptosis in malignant melanoma. *Oncogene.* 2006;25(4):512-524.
15. Wada T, Kikuchi J, Nishimura N, Shimizu R, Kitamura T, Furukawa Y. Expression levels of histone deacetylases determine the cell fate of hematopoietic progenitors. *J Biol Chem.* 2009; 284(44):30673-30683.
16. Somech R, Izraeli S, J Simon A. Histone deacetylase inhibitors: a new tool to treat cancer. *Cancer Treat Rev.* 2004;30(5):461-472.
17. Kim DH, Kim M, Kwon HJ. Histone deacetylase in carcinogenesis and its inhibitors as anti-cancer agents. *J Biochem Mol Biol.* 2003;36(1):110-119.
18. Hideshima T, Richardson P, Chauhan D, et al. The proteasome inhibitor PS-341 inhibits growth, induces apoptosis, and overcomes drug resistance in human multiple myeloma cells. *Cancer Res.* 2001;61(7):3071-3076.
19. Soucy TA, Smith PG, Milhollen MA, et al. An inhibitor of NEDD8-activating enzyme as a new approach to treat cancer. *Nature.* 2009; 458(7239):732-736.
20. Chauhan D, Catley L, Li G, et al. A novel orally active proteasome inhibitor induces apoptosis in multiple myeloma cells with mechanisms distinct from Bortezomib. *Cancer Cell.* 2005;8(5):407-419.
21. Annunziata CM, Davis RE, Demchenko Y, et al. Frequent engagement of the classical and alternative NF-κB pathways by diverse genetic abnormalities in multiple myeloma. *Cancer Cell.* 2007; 12(2):115-130.
22. Keats JJ, Fonseca R, Chesi M, et al. Promiscuous mutations activate the noncanonical NF-κB pathway in multiple myeloma. *Cancer Cell.* 2007; 12(2):131-144.
23. Hideshima T, Chauhan D, Richardson P, et al. NF-kappa B as a therapeutic target in multiple myeloma. *J Biol Chem.* 2002;277(19):16639-16647.
24. Hideshima T, Ikeda H, Chauhan D, et al. Bortezomib induces canonical NF-kappa B activation in multiple myeloma cells. *Blood.* 2009;114(5): 1046-1052.
25. Drexler HG, Matsuo Y, MacLeod RA. Persistent use of false myeloma cell lines. *Hum Cell.* 2003; 16(3):101-105.
26. Furukawa Y, Vu HA, Akutsu M, et al. Divergent cytotoxic effects of PKC412 in combination with conventional antileukemic agents in FLT3 mutation-positive versus -negative leukemia cell lines. *Leukemia.* 2007;21(5):1005-1014.
27. Kikuchi J, Shimizu R, Wada T, et al. E2F-6 suppresses growth-associated apoptosis of human hematopoietic progenitor cells by counteracting proapoptotic activity of E2F-1. *Stem Cells.* 2007; 25(10):2439-2447.
28. Sutheesophon K, Nishimura N, Kobayashi Y, et al. Involvement of the tumor necrosis factor (TNF)/TNF receptor system in leukemic cell apoptosis induced by histone deacetylase inhibitor depsipeptide (FK228). *J Cell Physiol.* 2005; 203(2):387-397.
29. Furukawa Y, Kikuchi J, Nakamura M, Iwase S, Yamada H, Matsuda M. Lineage-specific regulation of cell cycle control gene expression during haematopoietic cell differentiation. *Br J Haematol.* 2000;110(3):663-673.
30. Noborio-Hatano K, Kikuchi J, Takatoku M, et al. Bortezomib overcomes cell-adhesion-mediated drug resistance through downregulation of VLA-4 expression in multiple myeloma. *Oncogene.* 2009;28(2):231-242.
31. LeBlanc R, Catley LP, Hideshima T, et al. Proteasome inhibitor PS-341 inhibits human myeloma cell growth in vivo and prolongs survival in a murine model. *Cancer Res.* 2002;62(17): 4996-5000.
32. Chen J, Zhang M, Ju W, Waldmann TA. Effective treatment of a murine model of adult T-cell leukemia using depsipeptide and its combination with unmodified daclizumab directed toward CD25. *Blood.* 2009;113(6):1287-1293.
33. Piekarz RL, Robey R, Sandor V, et al. Inhibitor of histone deacetylation, depsipeptide (FR901228), in the treatment of peripheral and cutaneous T-cell lymphoma: a case report. *Blood.* 2001;98(9): 2865-2868.
34. Byrd JC, Marcucci G, Parthun M, et al. A phase I and pharmacodynamic study of depsipeptide (FK228) in chronic lymphocytic leukemia and acute myeloid leukemia. *Blood.* 2005;105(3):959-967.
35. Hideshima T, Bradner JE, Wong J, et al. Small-molecule inhibition of proteasome and aggresome function induces synergistic antitumor activity in multiple myeloma. *Proc Natl Acad Sci U S A.* 2005;102(24):8567-8572.
36. Shi J, Tricot GJ, Garg TK, et al. Bortezomib down-regulates the cell-surface expression of HLA class I and enhances natural killer cell-mediated lysis of myeloma. *Blood.* 2008;111(3):1309-1317.
37. Liu S, Liu Z, Xie Z, et al. Bortezomib induces DNA hypomethylation and silenced gene transcription by interfering with Sp1/NF-kappaB-dependent DNA methyltransferase activity in acute myeloid leukemia. *Blood.* 2008;111(4):2364-2373.
38. Chimienti F, Seve M, Richard S, Mathieu J, Favier A. Role of cellular zinc in programmed cell death: temporal relationship between zinc depletion, activation of caspases, and cleavage of Sp family transcription factors. *Biochem Pharmacol.* 2001; 62(1):51-62.
39. Hideshima T, Mitsiades C, Akiyama M, et al. Molecular mechanisms mediating antimyeloma activity of proteasome inhibitor PS-341. *Blood.* 2003;101(4):1530-1534.
40. Thorpe JA, Christian PA, Schwarze SR. Proteasome inhibition blocks caspase-8 degradation and sensitizes prostate cancer cells to death receptor-mediated apoptosis. *Prostate.* 2008;68(2): 200-209.
41. Landowski TH, Megli CJ, Nullmeyer KD, Lynch RM, Dorr RT. Mitochondrial-mediated disregulation of Ca^{2+} is a critical determinant of Velcade (PS-341/bortezomib) cytotoxicity in myeloma cell lines. *Cancer Res.* 2005;65(9):3828-3836.
42. Dolcet X, Llobet D, Pallares J. NF-κB in development and progression of human cancer. *Virchows Arch.* 2005;446(5):475-482.
43. Catley L, Weisberg E, Tai YT, et al. NVP-LAQ824 is a potent novel histone deacetylase inhibitor

with significant activity against multiple myeloma. *Blood.* 2003;102(7):2615-2622.

44. Miller CP, Rudra S, Keating MJ, Wierda WG, Palladino M, Chandra J. Caspase-8 dependent histone acetylation by a novel proteasome inhibitor, NPI-0052: a mechanism for synergy in leukemia cells. *Blood.* 2009;113(18):4289-4299.
45. Fotheringham S, Epping MT, Stimson L, et al. Genome-wide loss-of-function screen reveals an important role for the proteasome in HDAC inhibitor-induced apoptosis. *Cancer Cell.* 2009;15(1):57-66.
46. Mitsiades N, Mitsiades CS, Poulaki V, et al. Molecular sequelae of proteasome inhibition in human multiple myeloma cells. *Proc Natl Acad Sci U S A.* 2002;99(22):14374-14379.
47. Obeng EA, Carlson LM, Gutman DM, Harrington WJ, Lee KP, Boise LH. Proteasome inhibitors induce a terminal unfolded protein response in multiple myeloma cells. *Blood.* 2006;107(12):4907-4916.
48. Ogawa Y, Tobinai K, Ogura M, et al. Phase I and II pharmacokinetic and pharmacodynamic study of the proteasome inhibitor bortezomib in Japanese patients with relapsed or refractory multiple myeloma. *Cancer Sci.* 2008;99(1):140-144.
49. Rückrich T, Kraus M, Gogel J, et al. Characterization of the ubiquitin-proteasome system in bortezomib-adapted cells. *Leukemia.* 2009;23(6):1098-1105.
50. Bianchi G, Oliva L, Cascio P, et al. The proteasome load versus capacity balance determines apoptotic sensitivity of multiple myeloma cells to proteasome inhibition. *Blood.* 2009;113(13):3040-3049.

MSK1 activation in acute myeloid leukemia cells with FLT3 mutations

Leukemia (2010) **24,** 1087–1090; doi:10.1038/leu.2010.48;
published online 1 April 2010

FMS-like tyrosine kinase 3 (FLT3) is a member of class III receptor tyrosine kinases and is expressed on hematopoietic stem/progenitor cells. FLT3 is also expressed in the vast majority of acute myeloid leukemia (AML) cells and the expression levels are more abundant than those of normal hematopoietic stem/progenitor cells. In addition, FLT3 mutations, including internal tandem duplication of the juxtamembrane domain

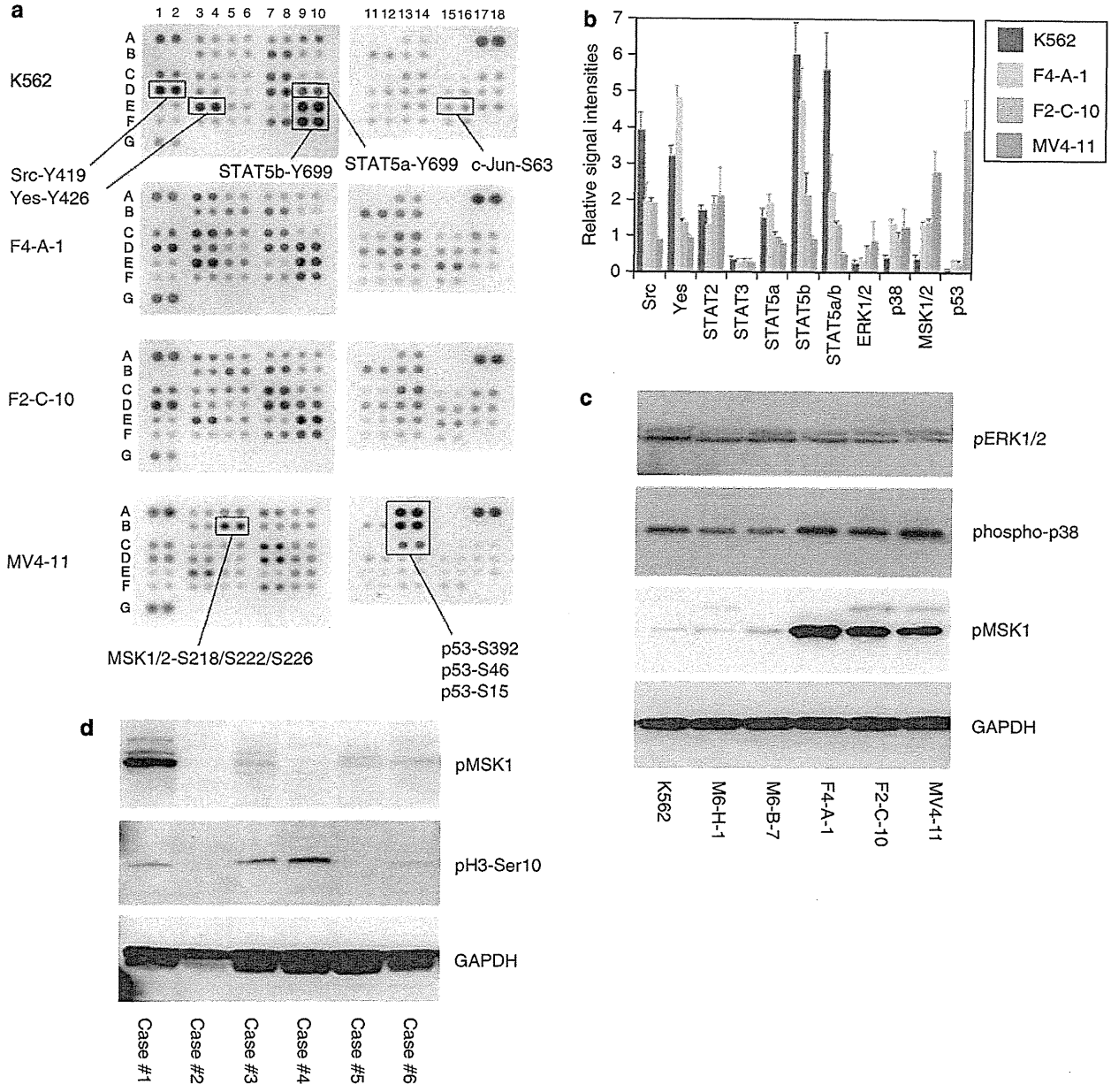

Figure 1 The presence of FLT3-ITD is associated with the activation of p38 MAP kinase-MSK1 axis. (**a**) Whole cell lysates were prepared from FLT3-ITD expressing K562 sublines (F4-A-1 and F2-C-10), K562 and MV4-11, and hybridized with a human Phospho-Kinase array according to the manufacturer's instructions. The locations of some molecules are annotated. See Supplementary Table S1 for complete listing. (**b**) Signal intensities of the indicated molecules were quantified using Scion Image software (Scion Corporation, Frederick, MD, USA), and normalized to those of positive controls on the same membrane (setting at 1.0). The means ± s.d. (bars) of two independent experiments are shown. (**c**) Whole cell lysates were prepared from K562 sublines, parental K562 and MV4-11, and subjected to immunoblot analysis for the expression of phosphorylated ERK1/2, phosphorylated p38 MAP kinase, phosphorylated MSK1, and GAPDH (internal control). Total ERK1/2, p38 and MSK1 were almost equally expressed in all samples, and thus, omitted from the blot. Data shown are representative of multiple independent experiments. (**d**) Whole cell lysates were isolated from primary AML samples, and subjected to immunoblot analysis for the expression of phosphorylated MSK1, phosphorylated histone H3 and GAPDH (internal control). Total MSK1 and histone H3 were almost equally expressed in all samples, and thus, omitted from the blot. Reverse transcriptase-PCR (RT-PCR) analysis revealed that cases 1, 3 and 6 were positive for FLT3-ITD (data not shown).

of FLT 3 (FLT3-ITD) and point mutations in the activating loop, are observed in approximately 30% of patients with AML. Given the great success of imatinib mesylate in chronic myeloid leukemia (CML), FLT3 inhibitors are expected to improve the treatment outcome of AML patients with FLT3 mutations.[1] Although the results of clinical trials as single agents are not satisfactory so far, more promising results have been achieved in combination with standard chemotherapy.[2] Therefore, FLT3 inhibitor-based treatment strategies would be more effective when combined with the drugs targeting downstream effectors of mutant FLT3.

To identify the critical downstream effectors of FLT3-ITD, we first analyzed biological consequences of the forced expression of FLT3-ITD in CML-derived K562 cell line. We established

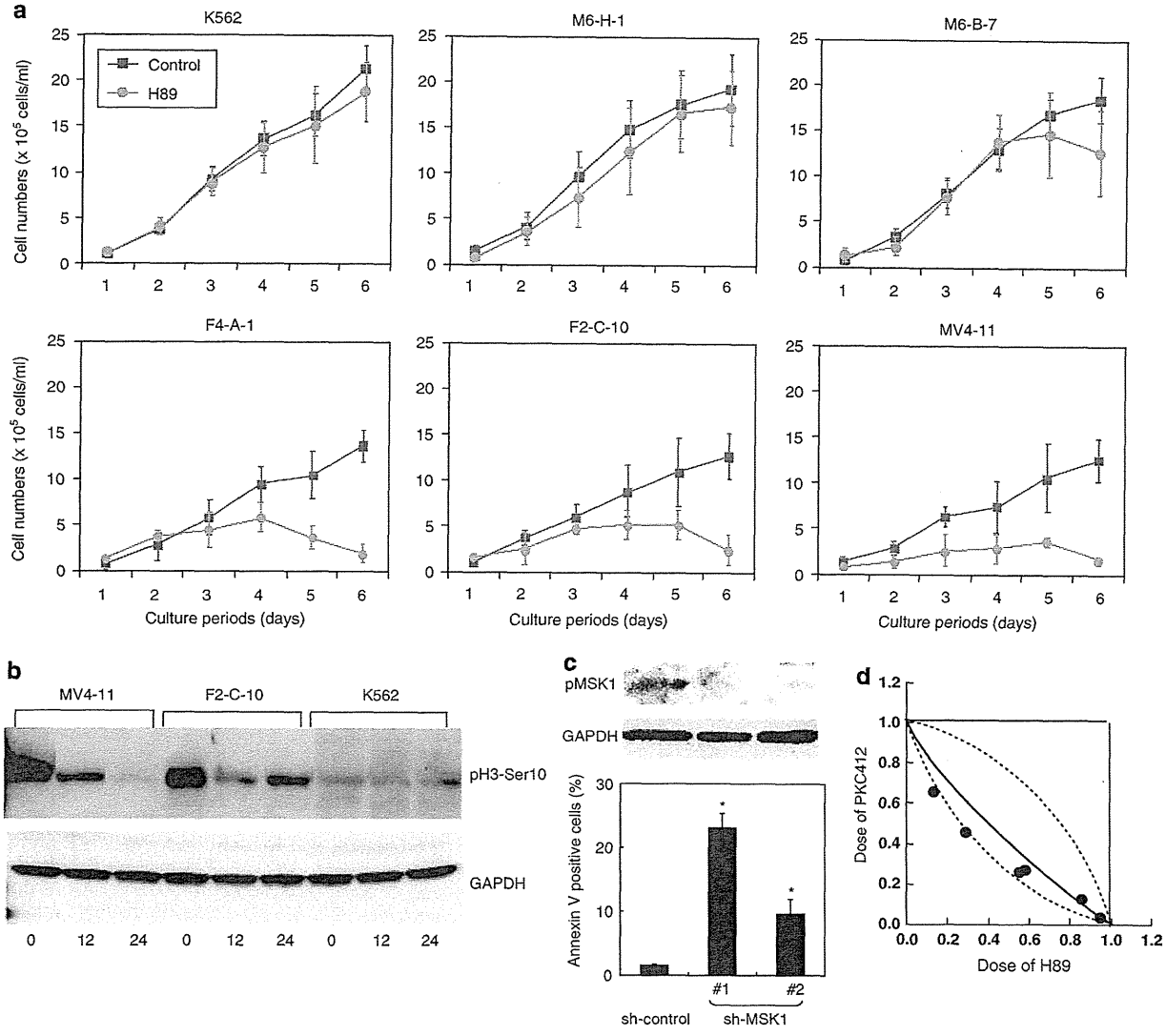

Figure 2 MSK1 inhibition results in growth suppression and apoptosis in AML cells carrying FLT3-ITD. (**a**) We seeded FLT3-ITD expressing K562 sublines, mock transfectants, K562 and MV4-11 at 1×10^5 cells/ml in RPMI1640 medium supplemented with 10% fetal calf serum, and cultured in the absence (control) or presence of 1 μM H89 (H89) for up to 6 days. Viable cells were counted after staining with erythrosine B dye. The means ± s.d. (bars) of five independent experiments are shown. (**b**) Whole cell lysates were prepared at the indicated time points, and subjected to immunoblot analysis for the expression of phosphorylated histone H3 and GAPDH (internal control). There was no change in the amounts of total histone H3 (data not shown). The data shown are representative of multiple independent experiments. (**c**) Upper panel; MV4-11 cells were transfected with either pLL3.7-sh-MSK1 (sh-MSK1) or sh-control (sh-control) vector. Whole cell lysates were prepared from green fluorescent protein (GFP)-positive cells collected using a FACSaria flow cytometer, and subjected to immunoblotting. Lower panel; MV4-11 cells transfected with short hairpin RNA (shRNA) vectors were cultured for 48 h, stained with annexin-V/APC, and subjected to flow cytometric analysis. The *y* axis shows the proportion of annexin-V positivity in the GFP-positive fraction. The means ± s.d. (bars) of three independent experiments are shown. *P*-values were calculated by one-way analysis of variance with the Student–Newman–Keuls multiple comparisons test. Asterisks indicate $P<0.05$ against the sh-control. (**d**) Isobologram analysis of the combination of PKC412 and H89 in MV4-11 cells. The theoretical basis of the isobologram method has been previously described in detail.[4] The concentrations that produced 80% growth inhibition are expressed as 1.0 on the ordinate and abscissa. The envelope of additivity, surrounded by solid and broken lines, is constructed from dose-response curves of H89 and PKC412. When the data points fall within the area surrounded by the envelope of additivity, the combination is regarded as additive. When the data points fall to the left and right of the envelope, the drug combination is regarded as supra-additive (synergism) and antagonistic, respectively. Each data point represents the mean value of at least three independent experiments; the s.e.m. were <25% and were omitted.

multiple stable transformants and verified the expression and phosphorylation of FLT3-ITD by immunoblotting. As shown in Supplementary Figure S1A, K562 sublines, F2-C-10 and F4-A-1, expressed FLT3-ITD at virtually identical levels to MV4-11. Importantly, FLT3-ITD was constitutively phosphorylated and thus was active in F2-C-10 and F4-A-1 cells, and constitutive phosphorylation of BCR-ABL was not impaired. Reflecting the dual expression of BCR-ABL and FLT3-ITD, these sublines responded to both imatinib and FLT3 inhibitors such as SU5416 and PKC412 (Supplementary Figure S1B).

Using these cell lines, we attempted to identify the signaling pathways preferentially activated by FLT3-ITD and BCR-ABL. To accomplish this, we isolated protein samples from FLT3-ITD expressing K562 sublines along with parental K562 and MV4-11 cells, and subjected them to human Phospho-Kinase array, which allows simultaneous determination of the activation status of 46 different protein kinases and their downstream effectors (see Supplementary Materials and Methods for detailed procedures; Figure 1a shows a representative blot). This approach revealed that FLT3-ITD and BCR-ABL activated differential signaling pathways: the mitogen-activated protein (MAP) kinase pathway, especially p38-MSK1 (mitogen- and stress-activated kinase 1) axis by FLT3-ITD; and the JAK-STAT pathway, especially JAK2-STAT5 axis by BCR-ABL, although there was some overlap (Figure 1b). It is noteworthy that FLT3-ITD expressing K562 sublines showed a pattern between parental cell lines MV4-11 and K562.

We then confirmed the results of Phospho-Kinase array with immunoblotting using antibodies different from those placed on the array. As shown in Figure 1c, MSK1 was exclusively phosphorylated in MV4-11 and FLT3-ITD expressing K562 sublines, and p38 MAP kinase was more abundantly phosphorylated in these cells than in K562 and mock-transfectants. Constitutive phosphorylation of MSK1 was also observed in another FLT3-ITD carrying cell line MOLM13 (data not shown). In contrast, no significant difference was observed in ERK1/2 phosphorylation in all cell lines examined. In addition, we examined MSK1 phosphorylation in primary AML samples from three FLT3-ITD-positive cases and three FLT3-ITD-negative cases including one case of CML-blastic crisis. As shown in Figure 1d, MSK1 phosphorylation was detected in all three FLT3-ITD-positive cases (cases 1, 3 and 6) and one FLT3-ITD-negative case (case 5), although there was a considerable case-to-case variation. MSK1 was not phosphorylated in other two FLT3-ITD-negative cases including the case with CML-blastic crisis (case 2). Constitutive activation of MSK1 was verified by monitoring the phosphorylation of histone H3 at serine-10, a canonical target site of MSK1.[3] H3-S10 phosphorylation was readily detected in all three FLT3-ITD-positive cases, although it was observed in case 4 independent of MSK1 activation.

Next, we analyzed whether MSK1 is indispensable for the maintenance of leukemic phenotype in AML cells carrying FLT3-ITD. To this end, we examined the effects of *N*-[2–p-bromocinnamylamino)ethyl]-5–isoquinolinesulfonamide (H89), a potent inhibitor of MSK1,[3] on cell growth of FLT3-ITD expressing K562 sublines and parental cell lines. As shown in Figure 2a, H89 inhibited the growth of FLT3-ITD expressing K562 sublines (F4-A-1 and F2-C-10) and MV4-11 cells but not K562 and mock-transfectants M6-H-1 and M6-B-7. The growth suppression became apparent 4–5 days after treatment with H89, and was due to the induction of apoptosis rather than cell cycle arrest (Supplementary Figure S2). The induction of apoptosis was accompanied by the reduced phosphorylation of H3-S10 (Figure 2b). As H89 inhibits not only MSK1 but also other kinases such as protein kinase A and ROCK-II, we took advantage of small interfering RNA-mediated knockdown to confirm that MSK1 is crucial for FLT3-ITD function (lentiviral vectors encoding short hairpin RNAs against MSK1 and scrambled controls were obtained from Open Biosystems, Huntsville, AL, USA). The numbers of apoptotic cells significantly increased along with the downregulation of MSK1 expression in MV4-11 (Figure 2c) and MOLM13 cells (data not shown) but not in K562 cells (data not shown). These results suggest that MSK1 is a critical downstream effecter of FLT3-ITD-mediated anti-apoptotic signal in AML cells.

Finally, we evaluated the cytotoxic interactions of H89 and PKC412 in MV4-11 cells using the isobologram of Steel and Peckham.[4] As anticipated, the two agents showed synergistic effects on MV4-11 and MOLM13 cells (Figure 2d and data not shown). In addition, H89 was also synergistic with another FLT inhibitor SU5416 (data not shown), suggesting that H89 and FLT3 inhibitors produce better effects in combination.

MSK1 was originally identified as a serine/threonine kinase activated by ERK1/2 and p38 in response to mitogenic stimuli as well as stress signals. Kim *et al.*[5] reported that H89 suppressed the transformation of murine epidermal cells by epidermal growth factor and 12-*O*-tetradecanoyl-phorbol-13-acetate, suggesting that MSK-1 is indispensable for carcinogenesis. Our findings suggest that the p38 MAP kinase-MSK1 axis also contributes to FLT3-ITD-mediated leukemogenesis. This is consistent with the previous observation that p38 is involved in cytokine-induced proliferation of an AML cell line.[6] In contrast, p38-MSK1 was not activated in CML-derived K562 cell line. Recently, it has been reported that the activation of p38 is essential for the effects of BCR-ABL inhibitors, implying that BCR-ABL promotes leukemogenesis via the suppression of the p38 MAP kinase pathway.[7,8] Taken together, these findings underscore the difference in the mechanisms of leukemogenesis by FLT3-ITD and BCR-ABL. Inhibition of the p38-MSK1 pathway might be an alternative for treatment of AML carrying FLT3 mutations.

Conflict of interest

The authors declare no conflict of interest.

T Odgerel[1,3], J Kikuchi[1,3], T Wada[1], R Shimizu[1], Y Kano[2] and Y Furukawa[1]
[1]*Division of Stem Cell Regulation, Center for Molecular Medicine, Jichi Medical School, Tochigi, Japan and* [2]*Division of Hematology, Tochigi Cancer Center, Tochigi, Japan*
E-mail: furuyu@jichi.ac.jp
[3]*These authors contributed equally to this work.*

References

1 Wadleigh M, DeAngelo DJ, Griffin JD, Stone RM. After chronic myelogenous leukemia: tyrosine kinase inhibitors in other hematologic malignancies. *Blood* 2005; **105**: 22–30.
2 Stone RM, DeAngelo DJ, Klimek V, Galinsky I, Estey E, Nimer SD *et al.* Patients with acute myeloid leukemia and an activating mutation in FLT3 respond to a small-molecule FLT3 tyrosine kinase inhibitor, PKC412. *Blood* 2005; **105**: 54–60.
3 Thomson S, Clayton AL, Hazzalin CA, Rose S, Barratt MJ, Mahadevan LC. The nucleosomal response associated with immediate-early gene induction is mediated via alternative MAP kinase cascades: MSK1 as a potential histone H3/HMG-14 kinase. *EMBO J* 1999; **18**: 4779–4793.

4 Furukawa Y, Vu HA, Akutsu M, Odgerel T, Izumi T, Tsunoda S *et al.* Divergent cytotoxic effects of PKC412 in combination with conventional antileukemic agents in FLT3 mutation-positive versus negative leukemia cell lines. *Leukemia* 2007; **21**: 1005–1014.
5 Kim H-G, Lee KW, Cho Y-Y, Kang NJ, Oh S-M, Bode AM *et al.* Mitogen- and stress-activated kinase 1-mediated histone H3 phosphorylation is crucial for cell transformation. *Cancer Res* 2008; **68**: 2538–2547.
6 Srinivasa SP, Doshi PD. Extracellular signal-regulated kinase and p38 mitogen-activated protein kinase pathways cooperate in mediating cytokine-induced proliferation of a leukemic cell line. *Leukemia* 2002; **16**: 244–253.
7 Parmar S, Katsoulidis E, Verma A, Li Y, Sassano A, Lal L *et al.* Role of the p38 mitogen-activated protein kinase pathway in the generation of the effects of imatinib mesylate (STI571) in BCR-ABL-expressing cells. *J Biol Chem* 2004; **279**: 25345–25352.
8 Dumka D, Puri P, Carayoi N, Balachandran H, Schuster K, Verma AK *et al.* Activation of the p38 MAP kinase pathway is essential for the antileukemic effects of dasatinib. *Leuk Lymphoma* 2009; **50**: 2017–2029.

Supplementary Information accompanies the paper on the Leukemia website (http://www.nature.com/leu)

CBL mutations in juvenile myelomonocytic leukemia and pediatric myelodysplastic syndrome

Leukemia (2010) **24,** 1090–1092; doi:10.1038/leu.2010.49; published online 1 April 2010

Juvenile myelomonocytic leukemia (JMML) is a rare form of myeloproliferative disorder, which is characterized by excessive myelomonocytic proliferation.[1] Gene mutations on RAS signaling pathways are a hallmark of JMML and are thought to be central to the pathogenesis of JMML. Mutations of *NF1*, *NRAS*, *KRAS* and *PTPN11* genes are found in approximately 70% of JMML patients, and are implicated in the aberrant RAS signaling.[1] On the other hand, the remaining approximately 30% of JMML patients have no known mutations.

In this regard, recent reports of somatic mutations of the *CBL* proto-oncogene in myeloid neoplasms are intriguing, because these *CBL* mutations were shown to result in aberrant tyrosine kinase signaling, which would lead also to activation of RAS signaling pathways.[2–4] We[2] and others[3,4] reported that *CBL* mutations occurred in a variety of myeloid neoplasms in adults, especially in chronic myelomonocytic leukemia,[2–4] which prompted us to search for possible *CBL* mutations in JMML cases as well as pediatric myelodysplastic syndrome (MDS) patients.

In total, 40 primary JMML and 24 pediatric MDS specimens were examined for CBL mutations. The median age at diagnosis of JMML was 1 year and 10 months (range, 2 months to 8 years and 4 months), and the study included 25 male and 15 female patients. MDS patients included 9 patients with refractory anemia, 14 with refractory anemia with excess of blasts and 1 with secondary MDS. As *CBL* mutations thus far reported almost exclusively involved exons 7–9 that encode linker/RING finger domains,[2–4] we confined our analysis to these exons using an ABI PRISM 310 Genetic Analyzer (Applied Biosystems, Branchburg, NJ, USA). Of the 40 JMML samples, 24 were also analyzed using Affymetrix GeneChip 250K *Nsp*I (Santa Clara, CA, USA).[5] Genome-wide detection of copy number abnormalities or allelic imbalances was performed using CNAG/AsCNAR software (http://www.genome.umin.jp),[5] which enabled sensitive detection of copy number neutral loss of heterozygosity (or acquired uniparental disomy (aUPD)).[5] Mutations of *RAS* and *PTPN11* were also examined as previously reported.[6] The study adhered to the principles of the Helsinki Declaration, and was conducted under the regulations enacted by the Ethics Board of Gunma Children's Medical Center.

CBL mutations were identified in 3 out of 40 JMML samples (7.5%), which were located in the linker sequence (Y371H in UPN1) or in the RING finger domain (C416Y in UPN18 and C419R in UPN38). The origin of the mutations has not been determined owing to the lack of appropriate normal tissues. All 3 *CBL*-mutated cases accompanied 11q-aUPD, whereas heterozygosity of 11q was preserved in the remaining 21 patients with wild-type *CBL*, recapitulating a strong association of *CBL* mutations with 11q-aUPD as previously described.[2] In UPN18, the chromatogram exclusively showed a mutated sequence, indicating that the mutation (C416Y) was homozygous. In the remaining patients, chromatograms were apparently heterozygous (Figure 1). Nevertheless, this did not necessarily exclude the possibility of homozygous mutations in the aUPD-positive cells, which were found in a small fraction within these tumor samples, as estimated from allele-specific copy numbers.

Recently, Loh *et al.*[7] have reported on *CBL* mutations in 27 (17%) of 159 JMML patients, which were exclusive with regard to *RAS/PTPN11* mutations. They also showed that Y371H mutations represented nearly 50% of all *CBL* mutations in JMML,[7] which were also found in a patient in our series. Mutations of *NRAS, KRAS* and *PTPN11* genes were found in 18, 10 and 34% of patients in our series, respectively, which did not co-exist with three *CBL* mutations (Table 1). In our study, no *CBL* mutations were found in 24 pediatric MDS patients. Combining both studies, the prevalence of *CBL* mutations is expected to be significantly lower in pediatric MDS patients than in JMML patients (0/24 vs 30/199; $P=0.025$), although the number of patients is still small.

CBL is a negative modulator of tyrosine kinase signaling and, as such, was demonstrated to act functionally and genetically as a tumor suppressor. On the other hand, CBL mutants in myeloid neoplasms have clear oncogenic properties, because they strongly transform fibroblasts. These CBL mutants inhibit the E3 ubiquitin ligase activity of both wild-type CBL and CBL-B, leading to prolonged tyrosine kinase activity after cytokine stimulation and hypersensitive proliferative responses of hematopoietic progenitors to a wide variety of cytokines.[8]

We have recently shown that the biological consequence of *CBL* mutations is prolonged activation of tyrosine kinases after cytokine/growth factor stimulations, which is further augmented under the *CBL*-null background as caused by aUPD.[2] Thus, *CBL* mutations associated with 11q-aUPD in JMML could provide a feasible explanation to the hypersensitivity to GM-CSF, which is

Leukemia (2010) 24, 1760–1768

www.nature.com/leu

ORIGINAL ARTICLE

HDAC inhibitors augment cytotoxic activity of rituximab by upregulating CD20 expression on lymphoma cells

R Shimizu[1,4], J Kikuchi[1,4], T Wada[1], K Ozawa[2], Y Kano[3] and Y Furukawa[1,2]

[1]*Division of Stem Cell Regulation, Center for Molecular Medicine, Jichi Medical University, Tochigi, Japan;* [2]*Division of Hematology, Department of Internal Medicine, Jichi Medical University, Tochigi, Japan and* [3]*Division of Hematology, Tochigi Cancer Center, Tochigi, Japan*

Anti-CD20 antibody rituximab is now essential for the treatment of CD20-positive B-cell lymphomas. Decreased expression of CD20 is one of the major mechanisms underlying both innate and acquired resistance to rituximab. In this study, we show that histone deacetylase (HDAC) inhibitors augment the cytotoxic activity of rituximab by enhancing the surface expression of CD20 antigen on lymphoma cells. HDAC inhibitors, valproic acid (VPA) and romidepsin, increased CD20 expression at protein and mRNA levels in B-cell lymphoma cell lines with relatively low CD20 expression levels. The VPA-mediated increase in CD20 expression occurred at 1 mM, which is clinically achievable and safe, but insufficient for inducing cell death. Chromatin immunoprecipitation assays revealed that HDAC inhibitors transactivated the *CD20* gene through promoter hyperacetylation and Sp1 recruitment. HDAC inhibitors potentiated the activity of rituximab in complement-dependent cytotoxic assays. In mouse lymphoma models, HDAC inhibitors enhanced CD20 expression along with histone hyperacetylation in transplanted cells, and acted synergistically with rituximab to retard their growth. The combination with HDAC inhibitors may serve as an effective strategy to overcome rituximab resistance in B-cell lymphomas.
Leukemia (2010) **24,** 1760–1768; doi:10.1038/leu.2010.157;
published online 5 August 2010
Keywords: rituximab; HDAC inhibitor; CD20; B-cell lymphoma; epigenetics; drug resistance

Introduction

Rituximab is a chimeric monoclonal antibody that binds to the pan-B-cell marker CD20, which is expressed in ~90% of B-cell lymphomas.[1] On engagement with CD20, rituximab kills target cells through complement-dependent cytotoxicity and antibody-dependent cellular cytotoxicity, as well as direct activation of the cell death program.[2] Since being approved for clinical use in 1997, rituximab has given great benefits to patients with B-cell lymphomas, and has changed the paradigm of the treatment of indolent lymphomas.[3,4]

Recently, rituximab resistance has emerged as an important clinical issue.[5] Although several mechanisms are proposed, loss of CD20 expression is undoubtedly one of the most straightforward and frequent causes of both innate and acquired resistance to rituximab in B-cell malignancies. It has been shown that the low response rate to rituximab is attributable to dim CD20 expression in chronic lymphocytic leukemia or small lymphocytic lymphoma[6] and Burkitt lymphoma.[7] In a cohort of diffuse large B-cell lymphoma, patients with low CD20 expression have a poor prognosis.[8] Furthermore, several cases of CD20-negative relapse were identified after treatment with rituximab-based regimens in diffuse large B-cell lymphoma.[9,10] Recently, Hiraga *et al.*[11] reported that relapse or disease progression was observed in ~30% of patients with B-cell lymphomas treated with rituximab-containing chemotherapies, and CD20 expression was lost in 5 of 19 relapsed patients who underwent repeated biopsy. It is of note that DNA-demethylating agents restored CD20 expression in lymphoma cells isolated from these patients, suggesting that epigenetic mechanisms underlie the downregulation of CD20 after rituximab treatment.

Epigenetics has a pivotal role in many pathological processes of cancer.[12] Accumulating evidence indicates that histone deacetylases (HDACs) are at the center of cancer epigenetics.[13] HDACs are a family of enzymes that catalyze the removal of acetyl groups from core histones, which results in chromatin compaction and transcriptional repression.[14] In leukemic cells, chromosomal translocation-generated fusion proteins, such as PML/RARα and AML-1/ETO, form a complex with HDACs, and aberrantly suppress the expression of genes required for cell differentiation and growth control, leading to the transformation of hematopoietic stem/progenitor cells.[13] In addition, HDAC overexpression is observed in various cancers, such as colon cancer,[15] malignant melanoma[16] and acute leukemia,[17] in association with histone hypoacetylation, which causes transcriptional repression of genes related to cell-cycle control, cell differentiation and apoptosis. Recent literature suggests that HDACs are also implicated in the drug resistance of B-cell malignancies such as multiple myeloma.[18,19]

Given the causative role of HDACs in cancer, small molecular inhibitors of HDACs are expected to constitute a novel class of anticancer drugs. HDAC inhibitors are able to restore the expression of genes that are aberrantly repressed in tumor cells, leading to cell-cycle arrest, differentiation and apoptosis.[20] In addition, it has been reported that HDAC inhibitors epigenetically modify the expression of cell surface molecules, such as tumor antigens (gp100[21] and NKG2D ligands[22]), death receptors (tumor necrosis factor receptor type I[23] and DR5[24]) and immunoregulatory molecules (CD86[25] and MHC II DRA[26]), in various tumors and immune effector cells. This property may broaden the application of HDAC inhibitors to the area of chemosensitization and cancer immunotherapy. In this study, we investigated whether HDAC inhibitors could enhance the expression of surface CD20 antigen on B-cell lymphoma cells to enforce the cytotoxic activity of rituximab.

Correspondence: Professor Y Furukawa, Division of Stem Cell Regulation, Center for Molecular Medicine, Jichi Medical University, 3311-1 Yakushiji, Shimotsuke, Tochigi 329-0498, Japan.
E-mail: furuyu@jichi.ac.jp
[4]These authors contributed equally to this work.
Received 12 October 2009; revised 6 May 2010; accepted 11 June 2010; published online 5 August 2010

Materials and methods

Cells and cell culture

We used five Burkitt lymphoma-derived cell lines (Daudi, BJA-B, Namalwa, Raji and Ramos), two diffuse large B-cell lymphoma cell lines (TK and B104) and a mantle lymphoma cell line (HBL-2) in this study. These cell lines were purchased from the Health Science Research Resources Bank (Osaka, Japan), except for HBL-2,[27] which was provided by Dr Masafumi Abe (Department of Pathology, Fukushima Medical University, Fukushima, Japan).

Drugs

HDAC inhibitors, valproic acid (VPA) and romidepsin (formerly known as FK228 or depsipeptide), were provided by Kyowa Hakko Kirin Co (Tokyo, Japan) and Gloucester Pharmaceuticals (Cambridge, MA, USA), respectively. We purchased rituximab from Zenyaku Kogyo Co (Tokyo, Japan).

Complement-dependent cytotoxicity assays

We carried out complement-dependent cytotoxicity assays as described by Stein *et al.*[28] with minor modifications. Cells were plated at 62 500 cells per well in black 96-well plates and incubated for 24 h with serially diluted rituximab in the presence of human complement (Quidel, SanDiego, CA, USA) at the final dilution of 1:4. Viable cell numbers were quantitatively measured with modified (3-(4,5-dimethylthiazol-2-yl)-2,5-diphenyltetrazolium) (MTT) assays using Cell Counting Kit-8 (Dojindo Molecular Technologies, Rockville, MD, USA).

Flow cytometry

We detected the surface expressions of CD20, CD10, CD21, CD43 and CD44 using specific antibodies against each molecule (eBioscience, San Diego, CA, USA) along with the corresponding isotype-matched controls using a FACSaria flow cytometer (Becton Dickinson, Bedford, MA, USA), as previously described.[29] We also used a phycoerythrin-conjugated annexin-V antibody (BD Biosciences, San Jose, CA, USA) for quantitative assessment of apoptosis.

Immunoblotting

Immunoblotting was carried out according to the standard method using anti-human CD20 monoclonal (clone 2H7; eBioscience) and anti-GAPDH polyclonal (Santa Cruz Biotechnology, Santa Cruz, CA, USA) antibodies.

Real-time quantitative reverse transcription PCR

Total cellular RNA was reverse-transcribed into cDNA using SuperScript reverse transcriptase and oligo(dT) primers (Invitrogen, Carlsbad, CA, USA), and subjected to real-time quantitative reverse transcription PCR using Power SYBR Green PCR Master Mix (Applied Biosystems, Warrington, UK) and the following primers: CD20 sense, 5′-ATGAAAGGCCCTATTGCTATG-3′; CD20 antisense, 5′-GCTGGTTCACAGTTGTATATG-3′. The data were quantified with the $2^{-\Delta\Delta Ct}$ method using simultaneously amplified GAPDH as a reference (primer sequences for GAPDH: sense, 5′-CCACCCATGGCAAATTCCATGGCA-3′; antisense, 5′-TCTAGACGGCAGGTCAGGTCCACC-3′).

Chromatin immunoprecipitation assays

We used the ChIP-IT chromatin immunoprecipitation kit (Active Motif, Carlsbad, CA, USA) for chromatin immunoprecipitation assays. In brief, cells were fixed with 1% formaldehyde at 37 °C for 5 min, and sonicated to obtain chromatin suspensions. After centrifugation, supernatants were incubated with either anti-acetyl histone H3 (Upstate Biotechnology/Millipore, Billerica, MA, USA), anti-Sp1 (Santa Cruz Biotechnology) or rabbit IgG at 4 °C overnight. The mixture was incubated with protein A agarose beads at 4 °C for 1 h, and centrifuged to collect the beads. DNA fragments bound to the beads were purified with vigorous washing, and subjected to PCR using primer pairs spanning −726 to −315 of the *CD20* gene.

Mouse lymphoma models

To establish mouse lymphoma models, we inoculated 3×10^6 lymphoma cells intravenously[30] or subcutaneously[19] into 6- to 8-week-old non-obese diabetic/severe combined immunodeficiency mice. Mice were assigned to four treatment groups receiving the vehicle (0.9% NaCl) plus mouse IgG, the vehicle plus rituximab, HDAC inhibitor plus mouse IgG, and HDAC inhibitor plus rituximab after 5 days in case of intravenous injection or when tumors were measurable in case of subcutaneous inoculation. We used either VPA (150 mg/kg twice a day) or romidepsin (0.1 mg/kg once a day) as an HDAC inhibitor. On the basis of previous studies,[30,31] rituximab was given through the tail vein at 25 mg/kg at 48 h after the administration of HDAC inhibitors. All animal studies were approved by the Animal Ethics Committee of Jichi Medical University, and performed in accordance with the Jichi Medical University Guide for Laboratory Animals, following the Guide for the Care and Use of Laboratory Animals formulated by the National Academy of Sciences.

Results

HDAC inhibitors enhance the expression of CD20 antigen on B-cell lymphoma cells

VPA is a short-chain fatty acid that has been used as an anticonvulsant over 40 years.[32] Recently, VPA was rediscovered as an HDAC inhibitor and has been tested in clinical trials for hematologic malignancies such as myelodysplastic syndrome and acute myeloblastic leukemia.[33,34] Unfortunately, VPA as a single agent is not so efficacious and so its combination with other drugs is under consideration. Given the ability of HDAC

Table 1 Time course of an increase in CD20 expression on lymphoma cells by valproic acid[a]

	Day 0	*Day 1*	*Day 2*	*Day 3*
HBL-2	99.3 ± 0.6	97.6 ± 2.4	95.3 ± 3.3	82.5 ± 5.6
TK	98.4 ± 0.8	95.6 ± 2.1	92.6 ± 4.8	88.6 ± 7.7
B104	28.5 ± 5.6	60.9 ± 1.4**	71.5 ± 2.0**	59.2 ± 13.2*
Daudi	39.4 ± 4.8	53.9 ± 9.9	76.1 ± 2.3**	81.0 ± 2.8**
BJA-B	16.8 ± 1.8	38.9 ± 21.5	59.6 ± 8.2**	88.0 ± 5.1**
Namalwa	25.2 ± 5.6	44.8 ± 5.2*	68.0 ± 9.3*	86.9 ± 13.6**
Raji	38.7 ± 9.4	55.5 ± 10.2	66.1 ± 7.7*	51.0 ± 12.3*
Ramos	29.1 ± 7.2	43.2 ± 7.6	56.8 ± 5.5*	61.7 ± 10.4*

[a]The proportion of CD20-positve cells was determined by comparison with the signal intensity of an isotype-matched control. Data are the means ± s.d. of three to five independent experiments.
P-values were calculated by one-way analysis of variance with the Bonferroni *post hoc* test (*$P<0.05$ and **$P<0.01$).

inhibitors to modulate the expression of various cell surface molecules,[21–26] we reasoned that VPA could enhance the expression of CD20 antigen on B-cell lymphoma cells, which would make VPA and rituximab an effective combination. As anticipated, VPA readily increased CD20 positivity and fluorescence intensity on five Burkitt lymphoma-derived cell lines and a diffuse large B-cell lymphoma cell line B104, in which CD20 expression was relatively low before treatment, but not in another diffuse large B-cell lymphoma cell line TK and a mantle lymphoma cell line HBL-2, which already expressed CD20 very strongly (Table 1, see Figures 1a and b for representative results). VPA elicited the effect very rapidly with a significant increase in CD20 being observed after 1–2 days of culture. It is of note that the enhancing effect was evident at 1 mM, a clinically achievable and safe concentration of VPA[35] (Table 2), whereas apoptosis of target cells was not clear at this concentration (Supplementary Figure S1 and Table S1). VPA-induced cell death required 2–5 mM, which apparently exceed the *in vivo* toxic concentrations, according to cumulative clinical data.[32,35] This at least partly explains why VPA failed to show considerable effects as a single agent in clinical trials.

We then examined whether another HDAC inhibitor romidepsin (formerly FK228 or depsipeptide) had the same effect. As shown in Table 3 (see Figures 1b and c for representative

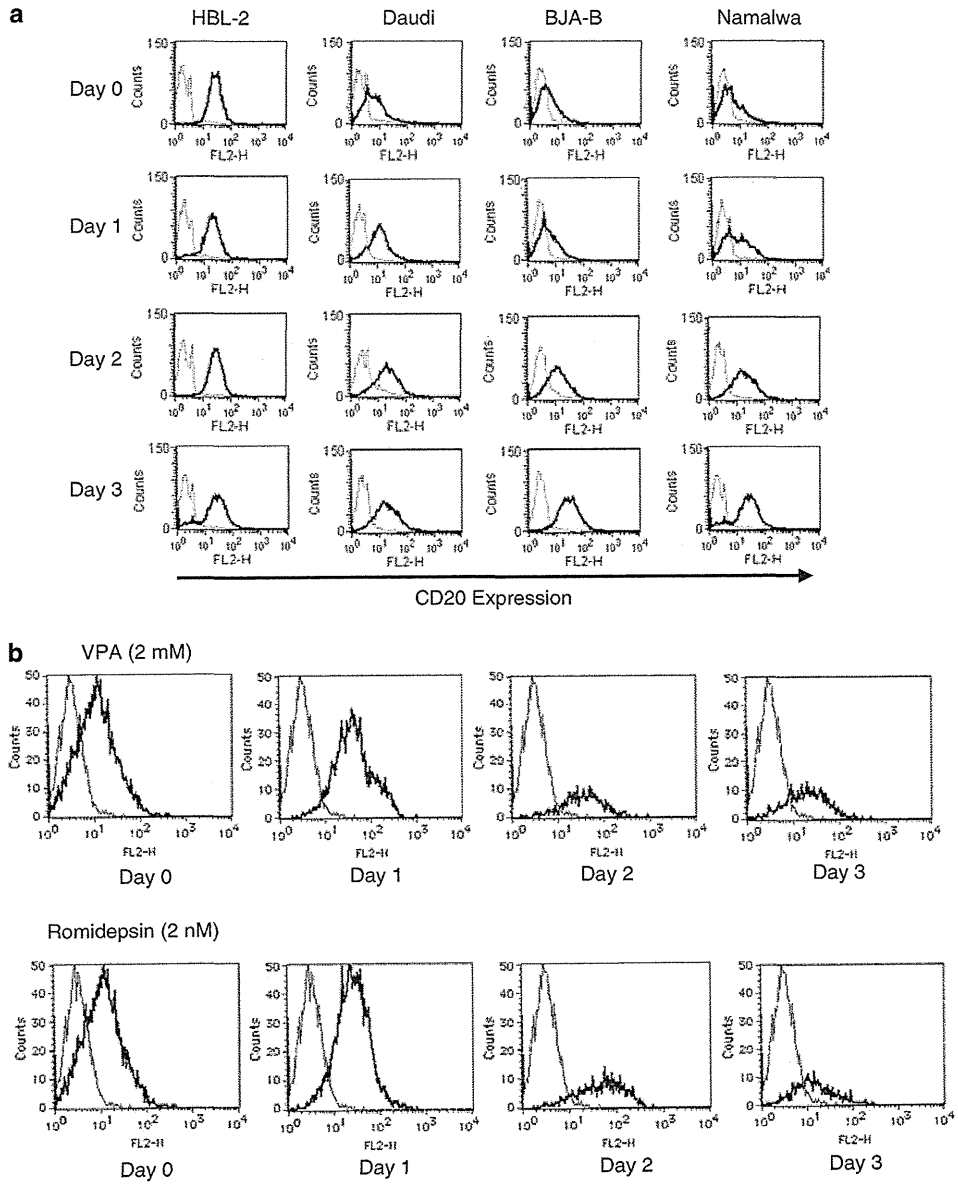

Figure 1 HDAC inhibitors enhance the expression of CD20 antigen on B-cell lymphoma cells. (**a**) B-cell lymphoma cell lines (HBL-2, Daudi, BJA-B and Namalwa) were cultured with 1 mM valproic acid, harvested at the indicated time points, and stained with either a phycoerythrin-conjugated anti-CD20 antibody (bold line) or mouse IgG2b isotype control (dotted line) in preparation for flow cytometry. (**b**) B104 cells were cultured with either 2 mM valproic acid or 2 nM romidepsin, harvested at the indicated time points, and stained with either a phycoerythrin-conjugated anti-CD20 antibody (bold line) or mouse IgG2b isotype control (thin line) in preparation for flow cytometry. (**c**) B-cell lymphoma cell lines (HBL-2, Daudi, BJA-B and Namalwa) were cultured with the indicated concentrations of romidepsin, harvested after 48 h, and stained with either a phycoerythrin-conjugated anti-CD20 antibody (bold line) or mouse IgG2b isotype control (dotted line) in preparation for flow cytometry.

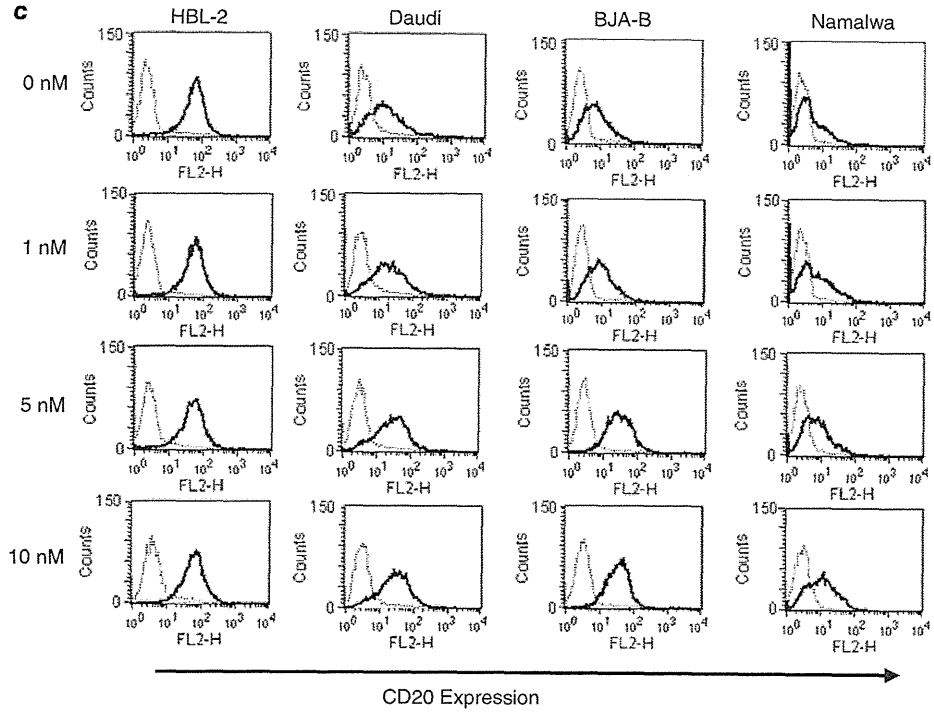

Figure 1 (continued).

Table 2 Dose-dependent increase in CD20 expression on lymphoma cells by valproic acid[a]

	0 mM	1 mM	2 mM	5 mM
HBL-2	95.4 ± 3.8	96.2 ± 5.7	82.7 ± 12.4	76.6 ± 29.3
TK	98.1 ± 0.9	93.2 ± 0.5	88.4 ± 10.4	86.6 ± 17.1
B104	28.5 ± 5.6	ND	71.5 ± 2.0*	ND
Daudi	39.6 ± 11.4	68.3 ± 11.7*	72.0 ± 17.7*	71.1 ± 13.8*
BJA-B	21.7 ± 16.3	72.9 ± 13.3**	80.3 ± 5.7*	86.4 ± 9.4**
Namalwa	25.7 ± 13.7	67.6 ± 9.8*	82.8 ± 13.2*	79.7 ± 10.8*
Raji	28.9 ± 9.8	58.9 ± 13.3*	88.6 ± 11.0*	72.9 ± 9.4*
Ramos	34.1 ± 12.6	55.8 ± 10.3	72.8 ± 11.5*	69.7 ± 10.8*

Abbreviation: ND, not done.
[a]The proportion of CD20-positve cells was determined by comparison with the signal intensity of an isotype-matched control. Data are the means ± s.d. of three to five independent experiments.
P-values were calculated by one-way analysis of variance with the Bonferroni *post hoc* test (*$P<0.05$ and **$P<0.01$).

Table 3 Dose-dependent increase in CD20 expression on lymphoma cells by romidepsin[a]

	0 nM	1 nM	5 nM	10 nM
B104	28.5 ± 5.6	ND	84.6 ± 4.8**	ND
Daudi	46.0 ± 5.8	56.3 ± 11.2	85.1 ± 3.3*	85.8 ± 2.0*
BJA-B	23.6 ± 9.8	38.9 ± 13.0	85.6 ± 13.1**	89.7 ± 9.8**
Namalwa	16.5 ± 6.3	32.3 ± 13.3*	78.9 ± 14.4**	83.3 ± 15.9**

Abbreviation: ND, not done.
[a]The proportion of CD20-positve cells was determined by comparison with the signal intensity of an isotype-matched control. Data are the means ± s.d. of three to five independent experiments.
P-values were calculated by one-way analysis of variance with the Bonferroni *post hoc* test (*$P<0.05$ and **$P<0.01$).

results), romidepsin significantly increased the surface expression of CD20 on Burkitt lymphoma and B104 cells at 5–10 nM, which were far lower than the maximum plasma concentration determined in phase I clinical trials (1.0–1.4 μM).[36–38] Romidepsin also had remarkable cytotoxic activities at the same concentrations (Supplementary Figure S2 and Table S2), consistent with the notion that this drug is one of the most effective HDAC inhibitors against hematological malignancies both *in vitro* and *in vivo*.[39,40] The upregulation of CD20 was not generalized to other B-cell-specific antigens, as the expression levels of CD10, CD21, CD43 and CD44 did not change in response to HDAC inhibitors (data not shown). This negates the possibility that HDAC inhibitors modify the expression of CD20 as a result of differentiation induction in lymphoma cells.

HDAC inhibitors transactivate the CD20 *gene through promoter acetylation and Sp1 recruitment*

We investigated the molecular mechanisms by which HDAC inhibitors enhanced the surface expression of CD20 antigen on lymphoma cells. First, we performed immunoblotting to examine whether HDAC inhibitors increased the abundance of CD20 protein in three Burkitt lymphoma cell lines and the B104 cell line. As shown in Figure 2a, the amounts of cellular CD20 protein readily increased after 24 h of culture with 1–2 mM VPA in all cell lines examined except for Daudi. In Daudi cells, VPA may facilitate the translocation of CD20 to the cell surface without an increase in protein synthesis as recently reported in certain settings,[41,42] although the mechanisms underlying this phenomenon are to be clarified. In contrast, HDAC inhibitors did not affect the expression levels of cellular CD20 protein in HBL-2 and TK cells, consistent with the results

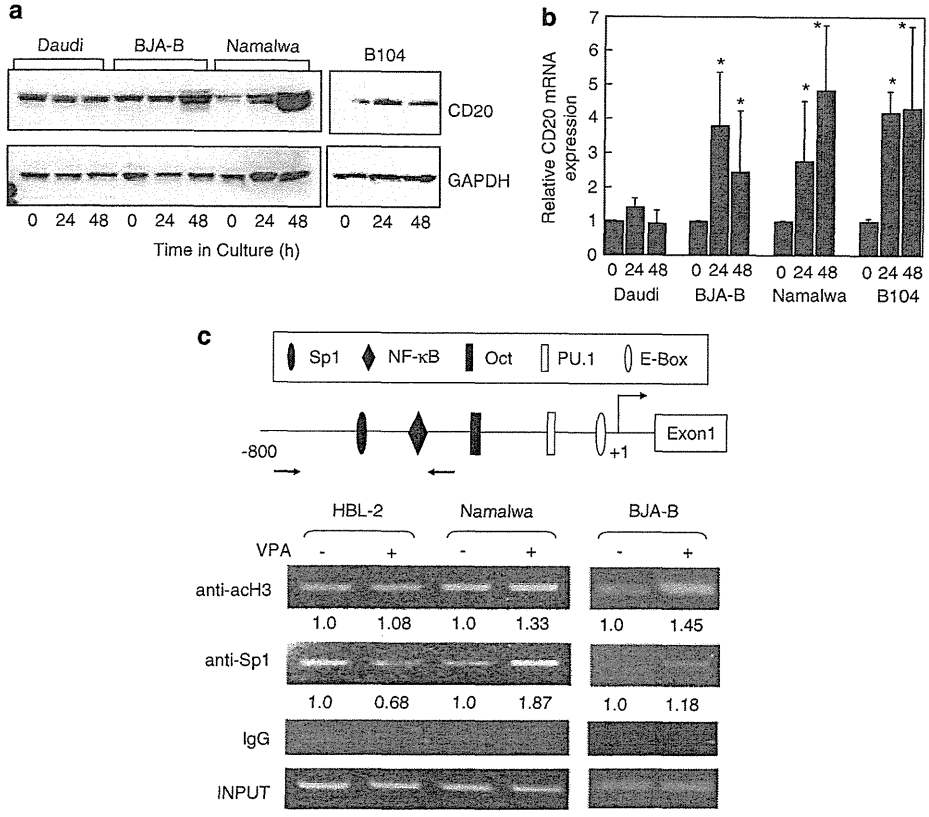

Figure 2 HDAC inhibitors transactivate the *CD20* gene through promoter acetylation and Sp1 recruitment. B-cell lymphoma cell lines (Daudi, BJA-B, Namalwa and B104) were cultured with 1 mM valproic acid for up to 48 h. We prepared whole-cell lysates and total cellular RNA at the indicated time points, and examined the expression of CD20 and GAPDH (internal control) using immunoblotting (**a**) and real-time quantitative RT-PCR (**b**). The results of real-time RT-PCR were quantified by the $2^{-\Delta\Delta Ct}$ method using *GAPDH* as a reference. Data shown are the means ± s.d. (bars) of three independent experiments. *P*-values were calculated by one-way analysis of variance with the Bonferroni *post hoc* test (*$P<0.05$). (**c**) Upper panel: A schematic representation of *CD20* promoter. Relative locations of the putative binding sites of transcription factors are approximated by the symbols shown in the box. See Supplementary Figure S5 for nucleotide sequences. Lower panel: Cells were cultured with valproic acid for 48 h, and harvested for chromatin immunoprecipitation assays. Chromatin suspensions were immunoprecipitated with the indicated antibodies and control IgG. The resulting precipitants were subjected to PCR to amplify the region indicated by arrows (−726 to −315). The amplified products were visualized by ethidium bromide staining after gel electrophoresis. Representative data of 40 cycles are shown. Input indicates that PCR was performed with genomic DNA. The signal intensities of each band were quantified, normalized to those of the corresponding input and shown as relative values setting untreated samples to 1.0.

of flow cytometry (data not shown). Next, we investigated whether HDAC inhibitors enhanced the expression of CD20 at mRNA levels. Both real-time quantitative reverse transcription PCR (Figure 2b) and Northern blotting (Supplementary Figure S3) revealed that *CD20* mRNA expression was significantly increased by VPA in BJA-B, Namalwa and B104 cells, but not in Daudi cells. These results are fully consistent with the results of immunoblotting, and suggest that VPA activates the transcription of the *CD20* gene to increase the abundance of CD20 protein in most cell lines. Romidepsin also increased the expression of CD20 at both protein and mRNA levels in BJA-B, Namalwa and B104 cells (Supplementary Figure S4 and data not shown).

To elucidate the mechanisms of *CD20* transactivation by HDAC inhibitors, we carried out chromatin immunoprecipitation assays on *CD20* promoter. As illustrated in Figure 2c, the 5′-untranslated region of the *CD20* gene contains canonical binding sites of Sp1 (−548 to −539; GC-Box), NF-κB (−425 to −417), Oct-1/Oct-2 (−214 to −199), PU.1/IRF4 (−161 to −148) and basic helix–loop–helix proteins (−45 to −40; E-Box) (see Supplementary Figure S5 for nucleotide sequences). Previous investigations have identified Oct-2, PU.1 and an E-Box-binding factor USF1 as positive regulatory elements, which confer lineage- and stage-specific expression of CD20 in B lymphocytes.[43,44] However, genetic studies using knockout mice indicate that Oct-2 is dispensable for early B-cell development and does not affect the baseline expression of CD20 in immature B lymphocytes.[45] In our pilot experiments, HDAC inhibitors reduced the expressions of PU.1 and USF1 to nearly undetectable levels (data not shown). We therefore focused on the region harboring the binding sites of Sp1 and NF-κB (−726 to −315) in this study. As shown in Figure 2c, VPA enhanced the acetylation of histone H3 in *CD20* promoter in BJA-B and Namalwa cells, but not in HBL-2 cells. Promoter acetylation coincided with the enhanced binding of Sp1, which may underlie the transcriptional activation of *CD20*. This notion is supported by the reduction of Sp1 binding to *CD20* promoter in VPA-treated HBL-2 cells, in which CD20 expression was slightly downregulated due to cytotoxic effects of VPA (Figure 1 and Table 1).

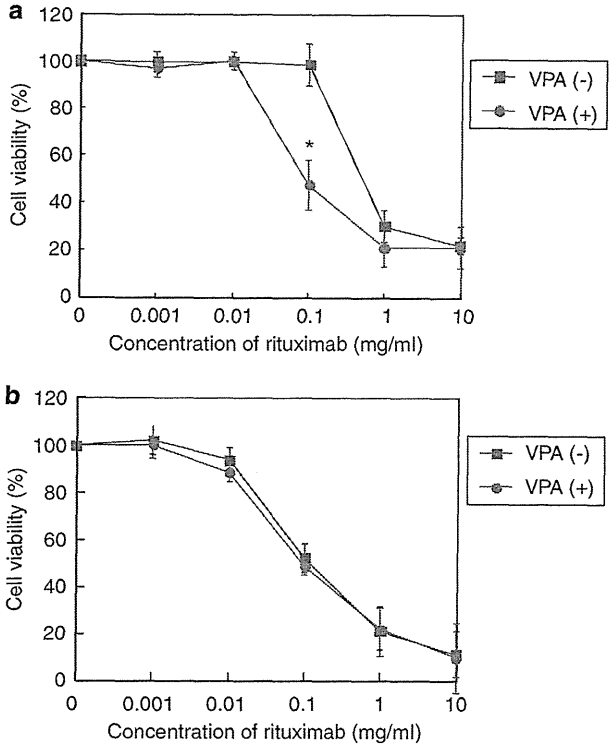

Figure 3 HDAC inhibitors augment the cytotoxic activity of rituximab *in vitro*. BJA-B (**a**) and HBL-2 (**b**) cells were pretreated with the vehicle (−) or VPA (+) for 48 h, washed, and further incubated for 24 h in the presence of human complement (1:4 dilution) and rituximab at the indicated concentrations. Cell viability was determined by modified MTT assays and shown as % untreated control. Each point represents the means ± s.d. (bars) of three independent experiments. *P*-values were calculated by paired Student's *t*-test (*$P<0.01$).

HDAC inhibitors enhance the cytotoxic effect of rituximab in vitro *and* in vivo

Finally, we examined whether the increased expression of CD20 was linked to the augmentation of the cytotoxic activity of rituximab. To this end, we first carried out *in vitro* complement-dependent cytotoxicity assays and found that HDAC inhibitors significantly enhanced the effect of rituximab at suboptimal concentrations (representative results of VPA-pretreated BJA-B cells are depicted in Figure 3a). The enhancement was not observed in HBL-2 and TK cells, in which HDAC inhibitors did not further increase CD20 expression (representative results of VPA-pretreated HBL-2 cells are depicted in Figure 3b). Next, we sought to determine whether this effect could be reproduced *in vivo* using mouse lymphoma models. First, we established lymphoma models by injecting BJA-B cells into non-obese diabetic/severe combined immunodeficiency mice intravenously. The mice were pretreated with either VPA or vehicle, followed by the administration of either rituximab or control IgG. Injected cells showed the enhancement of CD20 expression (Figure 4a) along with histone hyperacetylation (Figure 4b) *in vivo* after treatment with HDAC inhibitors. As expected, the increase in CD20 expression led to the enhancement of anti-lymphoma effects of rituximab; the numbers of CD45-positive cells were significantly lower in the bone marrow of mice pretreated with VPA (Figure 4c). However, VPA failed to prolong the survival of recipient mice compared with vehicle-treated control (data not shown). This might be due to neuronal toxicity of the drug, because VPA-treated mice showed a decrease in food intake and mobility. In addition, intravenously injected BJA-B cells seemed to grow too rapidly to be treated with rituximab alone. We therefore performed the *in vivo* experiment with the combination of another HDAC inhibitor romidepsin and subcutaneous inoculation of lymphoma cells. As shown in Figure 4d, the size of the subcutaneous tumor constantly increased in vehicle/IgG-treated control mice, and importantly, neither HDAC inhibitor alone nor rituximab alone inhibited tumor growth, consistent with the general consensus that Burkitt lymphoma is untreatable by these drugs as monotherapy.[3,4,7] In contrast, tumor growth was significantly retarded when two agents were combined (Figure 4d and Supplementary Figure S6). These results strongly suggest that HDAC inhibitors can potentiate the effects of rituximab *in vivo* by enhancing the expression of CD20.

Discussion

It is now widely accepted that rituximab is essential for the treatment of diffuse large B-cell lymphoma, follicular lymphoma and mantle cell lymphoma.[3,4] There are two emerging issues to be resolved for better usage of this drug: weak effects on some tumors[6–8] and drug resistance.[5,9–11] In this study, we clearly demonstrated that HDAC inhibitors, VPA and romidepsin, potentiated the cytotoxic effect of rituximab against Burkitt lymphoma, which has innate resistance to rituximab,[7] by enhancing the expression of surface CD20 antigen both *in vitro* and *in vivo*. We also analyzed the mechanisms of CD20 upregulation and found that HDAC inhibitors acetylated core histones of *CD20* promoter to enhance the binding of Sp1, leading to transactivation of the *CD20* gene in BJA-B and Namalwa cells. These results suggest that the innate resistance of these cells to rituximab is attributable to epigenetic silencing of CD20, which could be overcome by HDAC inhibitors. It is possible that the same mechanism also underlies acquired resistance in lymphomas heavily treated with rituximab. Indeed, Tomita *et al.*[46] have reported that an HDAC inhibitor, trichostatin A, could restore CD20 expression in a lymphoma cell line established from a patient with follicular lymphoma at the time of CD20-negative transformation after repeated treatment with rituximab. Taken together, HDAC inhibitors are promising agents to overcome both innate and acquired resistance to rituximab in patients with various B-cell malignancies.

HDAC inhibitors appear to upregulate the expression of CD20 specifically, because other B-cell markers such as CD10, CD21, CD43 and CD44 were unaffected. The mechanism underlying this specificity is not fully understood, but previous studies with regard to lineage-restricted expression of these molecules provide a plausible explanation. The expression of CD21 and CD44 was shown to be independent of Sp1,[47,48] a principal mediator of *CD20* transactivation by HDAC inhibitors. Transcription of *CD10* and *CD43* is governed by Sp1, but is also under the control of DNA methylation in a lineage-specific manner.[49,50] It is possible that Sp1 is not accessible to methylated *CD10* and *CD43* promoters of Burkitt lymphoma cells even after the treatment with HDAC inhibitors, although the involvement of other factors cannot be ruled out.

Owing to their unique mechanisms of action, HDAC inhibitors are expected to be effective for tumors resistant to conventional anticancer drugs, and indeed, exerted beneficial effects on peripheral T-cell lymphomas and malignant melanoma in experimental and pilot clinical studies.[16,40] However,

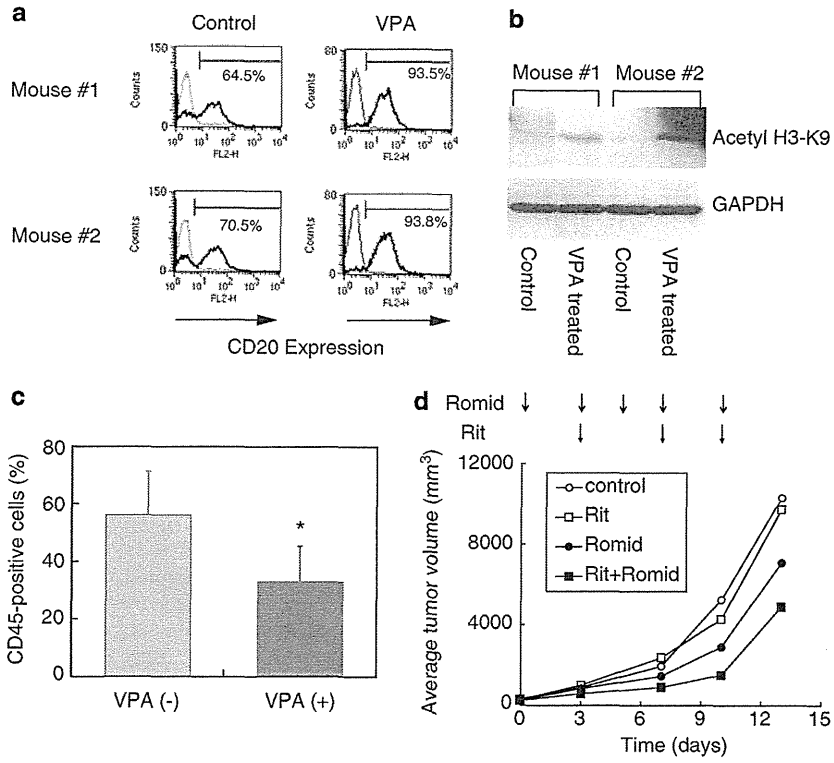

Figure 4 HDAC inhibitors augment the cytotoxic activity of rituximab *in vivo*. (**a**) We injected BJA-B cells into non-obese diabetic/severe combined immunodeficiency (NOD/SCID) mice intravenously, and treated them with the vehicle (control) or valproic acid at 150 mg/kg twice a day (VPA) from 4 days after transplantation. CD45-positive cells were isolated from the bone marrow of recipient mice after 48 h, and subjected to flow cytometric analysis for CD20 expression (**a**) and immunoblot analysis for histone H3 acetylation and GAPDH (**b**). (**c**) We determined the percentages of bone marrow CD45-positive cells using flow cytometry after 14 days of transplantation. The graph shows the means ± s.d. (bars) of samples from five mice. *P*-values were calculated by Student's *t*-test (**P*<0.05). (**d**) We inoculated Namalwa cells into the right flank of NOD/SCID mice, and started the following treatments when tumors were measurable (day 0): control (open circle), 0.9% NaCl on days 0, 3, 5, 7 and 10, followed by mouse IgG (25 mg/kg) on days 3, 7 and 10; rituximab alone (Rit, open square), 0.9% NaCl on days 0, 3, 5, 7 and 10, followed by rituximab (25 mg/kg) on days 3, 7 and 10; romidepsin alone (Romid, closed circle), romidepsin (0.1 mg/kg) on days 0, 3, 5, 7 and 10, followed by mouse IgG (25 mg/kg) on days 3, 7 and 10; romidepsin plus rituximab (Rit + Romid, closed square), romidepsin (0.1 mg/kg) on days 0, 3, 5, 7 and 10, followed by rituximab (25 mg/kg) on days 3, 7 and 10. Five mice were enrolled in each group. Caliper measurements of the longest perpendicular tumor diameters were performed every alternate day to estimate the tumor volume using the following formula: $4/3\pi \times (\text{width}/2)^2 \times (\text{length}/2)$, which represents the three-dimensional volume of an ellipse.

recent clinical trials concluded that HDAC inhibitors had only limited clinical activity when used as monotherapy.[33,34,36–38] Our present study suggests a more effective way of their application; the ability of HDAC inhibitors to modify the expression of surface molecules may provide a new avenue for the clinical application of HDAC inhibitors, for example, as immunopotentiators or chemosensitizers. Hence, the combination with HDAC inhibitors not only enhances anti-lymphoma activity, but also expands the clinical utility of rituximab for other disorders, such as autoimmune diseases.

Conflict of interest

The authors declare no conflict of interest.

Acknowledgements

This work was supported in part by the High-Tech Research Center Project for Private Universities: Matching Fund Subsidy from MEXT 2002-2006.

References

1 LeBien TW, Tedder TF. B lymphocytes: how they develop and function. *Blood* 2008; **112**: 1570–1580.
2 Bonavida B. Rituximab-induced inhibition of antiapoptotic cell survival pathways: implications in chemo/immunoresistance, rituximab unresponsiveness, prognostic and novel therapeutic interventions. *Oncogene* 2007; **26**: 3629–3636.
3 Coiffier B. Rituximab therapy in malignant lymphoma. *Oncogene* 2007; **26**: 3603–3613.
4 Cheson B, Leonard JP. Monoclonal antibody therapy for B-cell non-Hodgkin's lymphoma. *N Engl J Med* 2008; **359**: 613–626.
5 Smith MR. Rituximab (monoclonal anti-CD20 antibody): mechanisms of action and resistance. *Oncogene* 2003; **22**: 7359–7368.
6 Hainsworth JD, Litchy S, Barton JH, Houston GA, Hermann RC, Bradof JE *et al*. Single-agent rituximab as first-line and maintenance treatment for patients with chronic lymphocytic leukemia or small lymphocytic lymphoma: a phase II trial of the Minnie Pearl Cancer Research Network. *J Clin Oncol* 2003; **21**: 1746–1751.
7 Thomas DA, Faderl S, O'Brien S, Bueso-Ramos C, Cortes J, Garcia-Manero G *et al*. Chemoimmunotherapy with hyper-CVAD plus rituximab for the treatment of adult Burkitt and Burkitt-type lymphoma or acute lymphoblastic leukemia. *Cancer* 2006; **106**: 1569–1580.
8 Johnson NA, Boyle M, Bashashati A, Leach S, Brooks-Wilson A, Sehn LH *et al*. Diffuse large B-cell lymphoma: reduced CD20

expression is associated with an inferior survival. *Blood* 2009; **113**: 3773–3780.
9 Kennedy GA, Tey S-K, Cobcroft R, Marlton P, Cull G, Grimmett K *et al.* Incidence and nature of CD20-negative relapses following rituximab therapy in aggressive B-cell non-Hodgkin's lymphoma: a retrospective review. *Br J Haematol* 2002; **119**: 412–416.
10 Ferreri AJ, Dognini GP, Verona C, Patriarca C, Doglioni C, Ponzoni M. Re-occurrence of the CD20 molecule expression subsequent to CD20-negative relapse in diffuse large B-cell lymphoma. *Haematologica* 2007; **92**: e1–e2.
11 Hiraga J, Tomita A, Sugimoto T, Shimada K, Ito M, Nakamura S *et al.* Down-regulation of CD20 expression in B-cell lymphoma cells after treatment with rituximab-containing combination chemotherapies: its prevalence and clinical significance. *Blood* 2009; **113**: 4885–4893.
12 Esteller ME. Epigenetics in cancer. *N Engl J Med* 2008; **358**: 1148–1159.
13 Ropero S, Esteller M. The role of histone deacetylases (HDACs) in human cancer. *Mol Oncol* 2007; **1**: 19–25.
14 Yang X-J, Seto E. The Rpd3/Hda1 family of lysine deacetylases: from bacteria and yeast to mice and men. *Nat Rev Mol Cell Biol* 2008; **9**: 206–218.
15 Zhu P, Martin E, Mengwasser J, Schlag P, Janssen K-P, Gottlicher M. Induction of HDAC2 expression upon loss of APC in colorectal tumorigenesis. *Cancer Cell* 2004; **5**: 455–463.
16 Kobayashi Y, Ohtsuki M, Murakami T, Kobayashi T, Sutheesophon K, Kitayama H *et al.* Histone deacetylase inhibitor FK228 suppresses the Ras-MAP kinase signaling pathway by upregulating Rap1 and induces apoptosis in malignant melanoma. *Oncogene* 2006; **25**: 512–524.
17 Wada T, Kikuchi J, Nishimura N, Shimizu R, Kitamura T, Furukawa Y. Expression levels of histone deacetylases determine the cell fate of hematopoietic progenitors. *J Biol Chem* 2009; **284**: 30673–30683.
18 Maiso P, Carvajal-Vergara X, Ocio EM, Lopez-Perez R, Mateo G, Gutlerrez N *et al.* The histone deacetylase inhibitor LBH589 is a potent antimyeloma agent that overcomes drug resistance. *Cancer Res* 2006; **66**: 5781–5789.
19 Kikuchi J, Wada T, Shimizu R, Izumi T, Akutsu M, Mitsunaga K *et al.* Histone deacetylases are critical targets of bortezomib-induced cytotoxicity in multiple myeloma. *Blood,* e-pub ahead of print 29 March 2010; doi:10.1182/blood-2009-07-235663.
20 Xu WS, Parmigiani RB, Marks PA. Histone deacetylase inhibitors: molecular mechanisms of action. *Oncogene* 2007; **26**: 5541–5552.
21 Murakami T, Sato A, Chun NAL, Hara M, Naito Y, Kobayashi Y *et al.* Transcriptional modulation using HDACi depsipeptide promotes immune cell-mediated tumor destruction of murine B16 melanoma. *J Invest Dermatol* 2008; **128**: 1506–1516.
22 Diermayr S, Himmelreich H, Durovic B, Mathys-Schneeberger A, Siegler U, Langenkamp U *et al.* NKG2D ligand expression in AML increases in response to HDAC inhibitor valproic acid and contributes to allorecognition by NK-cell lines with single KIR-HLA class I specificities. *Blood* 2008; **111**: 1428–1436.
23 Sutheesophon K, Nishimura N, Kobayashi Y, Furukawa Y, Kawano M, Itoh K *et al.* Involvement of the tumor necrosis factor (TNF)/TNF receptor system in leukemic cell apoptosis induced by histone deacetylase inhibitor depsipeptide (FK228). *J Cell Physiol* 2005; **203**: 387–397.
24 Lundqvist A, Abrams SI, Schrump DS, Alvarez G, Suffredin D, Berg M *et al.* Bortezomib and depsipeptide sensitize tumors to tumor necrosis factor-related apoptosis-inducing ligand: a novel method to potentiate natural killer cell tumor cytotoxicity. *Cancer Res* 2006; **66**: 7317–7325.
25 Maeda T, Towatari M, Kosugi H, Saito H. Up-regulation of costimulatory/adhesion molecules by histone deacetylase inhibitors in acute myeloid leukemia cells. *Blood* 2000; **96**: 3847–3856.
26 Gialitakis M, Kretsovali A, Spilianakis C, Kravariti L, Mages J, Hoffmann R *et al.* Coordinated changes of histone modifications and HDAC mobilization regulate the induction of MHC class II genes by Trichostatin A. *Nucleic Acids Res* 2006; **34**: 765–772.
27 Suzuki O, Abe M. Cell surface *N*-glycosylation and sialylation regulate galectin-3-induced apoptosis in human diffuse large lymphoma. *Oncol Rep* 2008; **19**: 743–748.
28 Stein R, Qu Z, Chen S, Solis D, Hansen HJ, Goldenberg DM. Characterization of a humanized IgG4 anti-HLA-DR monoclonal antibody that lacks effector cell functions but retains direct antilymphoma activity and increases the potency of rituximab. *Blood* 2006; **108**: 2736–2744.
29 Kikuchi J, Shimizu R, Wada T, Ando H, Nakamura M, Ozawa K *et al.* E2F-6 suppresses growth-associated apoptosis of human hematopoietic progenitor cells by counteracting proapoptotic activity of E2F-1. *Stem Cells* 2007; **25**: 2439–2447.
30 Gillies SD, Lan Y, Williams S, Carr F, Forman S, Raubitschek A *et al.* An anti-CD20-IL-2 immunocytokine is highly efficacious in a SCID mouse model of established human B lymphoma. *Blood* 2005; **105**: 3972–3978.
31 Bertolini F, Fusetti L, Mancuso P, Gobbi A, Corsini C, Ferrucci PF *et al.* Endostatin, an antiangiogenic drug, induces tumor stabilization after chemotherapy or anti-CD20 therapy in a NOD/SCID mouse model of human high-grade non-Hodgkin lymphoma. *Blood* 2000; **96**: 282–287.
32 Haddad PM, Das A, Ashfaq M, Wieck A. A review of valproate in psychiatric practice. *Expert Opin Drug Metab Toxicol* 2009; **5**: 539–551.
33 Kuendgen A, Strupp C, Aivado M, Bernhardt A, Hildebrandt B, Haas R *et al.* Treatment of myelodysplastic syndromes with valproic acid alone or in combination with all-*trans* retinoic acid. *Blood* 2004; **104**: 1266–1269.
34 Kuendgen A, Schmid M, Schlenk R, Knipp S, Hildebrandt B, Steidl C *et al.* The histone deacetylase (HDAC) inhibitor valproic acid as monotherapy or in combination with all-trans retinoic acid in patients with acute myeloid leukemia. *Cancer* 2006; **106**: 112–119.
35 Tisdale JE, Tsuyuki RT, Oles KS, Penry JK. Relationship between serum concentration and dose of valproic acid during monotherapy in adult outpatients. *Ther Drug Monitor* 1992; **14**: 416–423.
36 Bryd JC, Marcucci G, Parthum MR, Xiao JJ, Klisovic RB, Moran M *et al.* A phase 1 and pharmacodynamic study of depsipeptide (FK228) in chronic lymphocytic leukemia and acute myeloid leukemia. *Blood* 2005; **105**: 959–967.
37 Fouladi M, Furman WL, Chin T, Freeman III BB, Dudkin L, Stewart CF *et al.* Phase I study of depsipeptide in pediatric patients with refractory solid tumors: a children's oncology group report. *J Clin Oncol* 2006; **24**: 3678–3685.
38 Klimek VN, Fircanis S, Maslak P, Guernah I, Baum M, Wu N *et al.* Tolerability, pharmacodynamics, and pharmacokinetics studies of depsipeptide (romidepsin) in patients with acute myelogenous leukemia or advanced myelodysplastic syndromes. *Clin Cancer Res* 2008; **14**: 826–832.
39 Sutheesophon K, Kobayashi Y, Takatoku M, Ozawa K, Kano Y, Furukawa Y. Histone deacetylase inhibitor depsipeptide (FK228) induces apoptosis in leukemic cells by facilitating mitochondrial translocation of Bax, which is enhanced by the proteasome inhibitor bortezomib. *Acta Haematol* 2006; **115**: 78–90.
40 Piekarz RL, Robey R, Sandor V, Bakke S, Wilson WH, Dahmoush L *et al.* Inhibitor of histone deacetylation, depsipeptide (FR901228), in the treatment of peripheral and cutaneous T-cell lymphoma: a case report. *Blood* 2001; **98**: 2865–2868.
41 Jilani I, O'Brien S, Manshuri T, Thomas DA, Thomazy VA, Imam M *et al.* Transient down-modulation of CD20 by rituximab in patients with chronic lymphocytic leukemia. *Blood* 2003; **102**: 3514–3520.
42 Lapalombella R, Yu B, Triantafillou G, Liu Q, Butchar JP, Lozanski G *et al.* Lenalidomide down-regulates the CD20 antigen and antagonizes direct and antibody-dependent cellular cytotoxicity of rituximab on primary chronic lymphocytic leukemia cells. *Blood* 2008; **112**: 5180–5189.
43 Thevenin C, Lucas BP, Kozlow EJ, Kehrl JH. Cell type- and stage-specific expression of the CD20/B1 antigen correlates with the activity of a diverged octamer DNA motif present in its promoter. *J Biol Chem* 1993; **268**: 5949–5956.
44 Himmelmann A, Riva A, Wilson GL, Lucas BP, Thevenin C, Kehrl JH. PU.1/Pip and basic helix loop helix zipper transcription factors interact with binding sites in the CD20 promoter to help confer lineage- and stage-specific expression of CD20 in B lymphocytes. *Blood* 1997; **90**: 3984–3995.

45 Corcoran LM, Karvelas M, Nossal GJV, Ye Z-S, Jacks T, Baltimore D. Oct-2, although not required for early B-cell development, is critical for later B-cell maturation and for postnatal survival. *Genes Dev* 1993; **7**: 570–582.
46 Tomita A, Hiraga J, Kiyoi H, Ninomiya M, Sugimoto T, Ito M *et al.* Epigenetic regulation of CD20 protein expression in a novel B-cell lymphoma cell line, RRBL1, established from a patient treated repeatedly with rituximab-containing chemotherapy. *Int J Hematol* 2007; **85**: 49–57.
47 Cruickshank MN, Fenwick E, Karimi M, Abraham LJ, Ulgiati D. Cell- and stage-specific chromatin structure across the complement receptor 2 (*CR2/CD21*) promoter coincide with CBF1 and C/EBP-β binding in B cells. *Mol Immunol* 2009; **46**: 2613–2622.
48 Maltzman JS, Carman JA, Monroe JG. Transcriptional regulation of the *Icam-1* gene in antigen receptor- and phorbol ester-stimulated B lymphocytes: Role for transcription factor EGR1. *J Exp Med* 1996; **183**: 1747–1759.
49 Ikawa Y, Sugimoto N, Koizumi S, Yachie A, Saikawa Y. Dense methylation of types 1 and 2 regulatory regions of the CD10 gene promoter in infant acute lymphoblastic leukemia with MLL/AF4 fusion gene. *J Pediatr Hematol Oncol* 2010; **32**: 4–10.
50 Kudo S. Methyl-CpG-binding protein MeCP2 represses Sp1-activated transcription of the human leukosialin gene when the promoter is methylated. *Mol Cell Biol* 1998; **18**: 5492–5499.

Supplementary Information accompanies the paper on the Leukemia website (http://www.nature.com/leu)

Int J Hematol (2010) 91:284–292
DOI 10.1007/s12185-009-0483-2

ORIGINAL ARTICLE

Allogeneic stem cell transplantation versus chemotherapy as post-remission therapy for intermediate or poor risk adult acute myeloid leukemia: results of the JALSG AML97 study

Hisashi Sakamaki · Shuichi Miyawaki · Shigeki Ohtake · Nobuhiko Emi · Fumiharu Yagasaki · Kinuko Mitani · Shin Matsuda · Yuji Kishimoto · Yasushi Miyazaki · Norio Asou · Masatomo Takahashi · Yoshiaki Ogawa · Sumihisa Honda · Ryuzo Ohno

Received: 13 May 2009 / Revised: 4 December 2009 / Accepted: 22 December 2009 / Published online: 9 January 2010

Abstract We prospectively compared allogeneic hematopoietic stem cell transplantation (allo-HSCT) with chemotherapy as a post-remission therapy in a multicenter trial (JALSG AML97) of adult patients with intermediate or poor risk acute myeloid leukemia (AML). Of 503 patients aged 15–50 years old registered between December 1997 and July 2001, 392 achieved complete remission (CR). CR patients classified in the intermediate or poor risk group using a new scoring system were tissue typed. Seventy-three with and 92 without an HLA-identical sibling were assigned to the donor and no-donor groups. Of 73 patients in the donor group, 38 (52%) received allo-HSCT during CR1 and 17 (23%) after relapse. Intention-to-treat analysis revealed that the relapse incidence was reduced in the donor group (52 vs. 77%; $p = 0.008$), and the disease-free survival (DFS) improved (39 vs. 19%; $p = 0.016$), but overall survival (OS)

For the Japan Adult Leukemia Study Group (JALSG).

H. Sakamaki (✉)
Division of Hematology, Tokyo Metropolitan Komagome Hospital, 3-18-22 Honkomagome, Bunkyo-ku, Tokyo 113-8677, Japan
e-mail: sakamaki-h@cick.jp

S. Miyawaki
Division of Hematology, Tokyo Metropolitan Ohtsuka Hospital, Tokyo, Japan

S. Ohtake
Department of Clinical Laboratory Science, Kanazawa University Graduate School of Medical Science, Kanazawa, Japan

N. Emi
Department of Hematology, Fujita Health University, Aichi, Japan

F. Yagasaki
Department of Internal Medicine (Hematology), Saitama Medical School, Saitama, Japan

K. Mitani
Department of Hematology, Dokkyo University School of Medicine, Tochigi, Japan

S. Matsuda
Center for Hematopoietic Disorders, Ohtanisinouchi Hospital, Kohriyama, Japan

Y. Kishimoto
The First Department of Internal Medicine, Kansai Medical University, Osaka, Japan

Y. Miyazaki
The Department of Hematology, Atomic Bomb Disease Institute, Nagasaki University School of Medicine, Nagasaki, Japan

N. Asou
Department of Hematology, Kumamoto University School of Medicine, Kumamoto, Japan

M. Takahashi
Division of Hematology and Oncology, Department of Internal Medicine, St. Marianna University School of Medicine, Kawasaki, Japan

Y. Ogawa
Department of Hematology and Oncology, Tokai University School of Medicine, Kanagawa, Japan

S. Honda
Department of Radiation Epidemiology, Atomic Bomb Disease Institute, Nagasaki University School of Medicine, Nagasaki, Japan

R. Ohno
Aichi Cancer Center, Aichi, Japan

was not significantly different (46 vs. 29%; $p = 0.088$). The OS benefit was seen in the patients aged 36–50 years old (49 vs. 24%; $p = 0.031$), suggesting an advantage of allo-HSCT among older patients with leukemia that is more resistant to chemotherapy than that among younger patients.

Keywords AML · Allogeneic hematopoietic stem cell transplantation · Post-remission chemotherapy

1 Introduction

Around 70–80% of newly diagnosed patients with adult acute myeloid leukemia (AML) achieve complete remission (CR) when treated with cytarabine (AraC) and anthracycline, usually daunorubicin (DNR) or idarubicin (IDR). However, only about one-third of these patients remain disease free for more than 5 years [1–5]. Intensified post-remission chemotherapy has improved the survival rates of patients with AML, especially of younger patients [6]. Allogeneic hematopoietic stem cell transplantation (allo-HSCT) is considered to be the most intensive post-remission treatment consisting of high-dose chemoradiotherapy and allo-immune mechanisms. However, the powerful anti-leukemic effects of this treatment are counterbalanced by a high incidence of treatment-related mortality (TRM). Thus, allo-HSCT has not always been considered superior to chemotherapy [7, 8]. Intensified chemotherapy with high-dose Ara-C confers promising results on good risk patients [9] for whom allo-HSCT is currently abstained in the first CR (CR1). The Japan Adult Leukemia Study Group (JALSG) AML97 protocol committee circulated a questionnaire among the institutions participating in JALSG regarding their policy about indications for allo-HSCT among AML patients in CR1. The findings revealed that good risk patients in CR1 did not undergo an allo-HSCT at most of these institutions. Cytogenetic profile has been widely used to classify the patients with AML [7–13]; however, cytogenetic studies are not always foolproof. The JALSG established a scoring system that adopted significant factors including cytogenetic results from previous JALSG AML trials [14]. We applied this scoring system to stratify patients and conducted a prospective, multicenter cooperative study (AML97) to compare allo-HSCT with chemotherapy among intermediate and poor risk patients with AML in CR1.

2 Patients and methods

2.1 Patients and study design

The JALSG AML97 study was implemented between December 1997 and July 2001 at 103 institutions where the ethical committees approved the protocol. Adult patients aged from 15 to 64 years newly diagnosed with de novo AML according to the French–American–British (FAB) classification at each institution were eligible, but those with acute promyelocytic leukemia (APL) were excluded. Peripheral blood and bone marrow smears of the registered patients were stained with May-Giemsa, peroxidase, and esterase at Nagasaki University and subsequently reviewed by a central review committee. All patients provided written informed consent to participate before registration in this study.

The chemotherapeutic design of AML97 has been described elsewhere in detail [15]. In short, all the patients were treated with the same induction therapy consisted of AraC (100 mg/m^2, continuous infusion, days 1–7) and IDR (12 mg/m^2 days 1–3). If the patients did not achieve remission after the first induction therapy, then the same therapy was given again. For patients who did not achieve a CR even after second induction therapy, no further treatment was defined in this study. In the comparison between allo-HSCT and chemotherapy as post-remission therapy, these patients were not included in the analysis. All patients who achieved CR were randomized to receive either 4 courses of consolidation therapy without maintenance therapy (group A) or the conventional JALSG post-remission regimen with maintenance therapy (group B) [3]. The results of the two post-remission chemotherapeutic strategies (group A vs. group B) were comparable [15]. The CR patients were classified into good, intermediate or poor risk groups according to the scoring system described below. Intermediate or poor risk patients younger than 50 years old with living siblings were tissue typed. Patients with an HLA-identical sibling were assigned to undergo allo-HSCT soon after three courses of consolidation therapy (donor group), and those without living or HLA-identical siblings were assigned to the no-donor group that continued receiving chemotherapy.

Patients in the donor group with AST or ALT values fourfold higher than the normal range, serum bilirubin and creatinine more than 2 mg/dl, ejection fraction based on an echocardiogram of less than 50% or oxygen saturation according to pulse oximetry of less than 90% were ineligible for allo-HSCT, but were analyzed as a donor group one in an intention-to-treat fashion. Conditioning before transplantation and prophylaxis for graft-versus-host disease was performed according to each institutional standard. Either allogeneic peripheral blood or bone marrow was allowed to be the stem cell source.

2.2 Scoring system

We collected clinical and laboratory data (except for APL) from previous JALSG AML trials (AML87, $n = 234$

Table 1 JALSG scoring system

Scoring system		
System 1		
MPO positive blasts	>50%	+2
Age	≤50 years	+2
WBC	$\leq 2 \times 10^9$/l	+2
FAB subtypes	non-M0, M6, M7	+1
Performance status	0, 1, 2	+1
No. of induction	1	+1
t(8;21) or inv(16)	+	+1
Total score		
Good risk group		8–10
Intermediate risk group		5–7
Poor risk group		0–4
System 2		
MPO positive blasts	>50%	+2
Age	≤50 years	+2
WBC	$\leq 2 \times 10^9$/l	+2
FAB subtypes	non-M0, M6, M7	+1
Performance status	0, 1, 2	+1
Total score		
Good risk group		7–8
Intermediate risk group		4–6
Poor risk group		0–3

MPO myeloperoxidase, *WBC* white blood cell

patients; AML89, $n = 311$; AML92, $n = 986$), and then selected significant factors for achieving CR, disease-free survival (DFS) and overall survival (OS) using multivariate analysis [14]. According to the weight of significance, myeloperoxidase positivity of blasts, patient age, and WBC count at diagnosis were valued at 2 points, and FAB subtypes, performance status, numbers of inductions required to achieve CR, and favorable karyotypes of t(8;21) or inv(16) were valued at 1 point (Table 1, system 1). When we originally planned to use this system, cytogenetic data were not always available at diagnosis. Thus, we designed the system 2 that could be applied even without a cytogenetic data.

2.3 Statistical analysis

The aim of this study was to compare the efficacy of allo-HSCT and chemotherapy as a post-remission treatment, by evaluating DFS and OS rate. Forty-two patients were estimated for an evaluation of the primary endpoint of this study. The JALSG data management committee collected the clinical data from all participating institutions, then fixed them and analyzed the OS of each risk group in July 2004 and the relapse rate (RR), DFS, OS and TRM of the donor and no-donor groups in January 2009. The OS, DFS, RR and TRM were measured from the date of CR. The event for OS was death due to all causes, and patients were censored at the last observation date if alive. The events of DFS were death during CR or relapse. The RR was defined as the cumulative probability of relapse, censoring at death in CR. The events of TRM comprised death before relapse. We estimated OS, DFS, RR and TRM with their respective standard errors using the Kaplan–Meier method [16]. We compared the OS, DFS, RR and TRM between the patients with and without a donor using the log-rank test. Furthermore, the hazard ratio and the 95% confidence interval (CI) of the OS, DFS, RR and TRM were calculated using Cox regression analysis. The Wilcoxon rank-sum test was used for the continuous data, such as age and WBC count, while the Chi-square test was used for the ordinal data, such as the risk group and the frequency of allo-HSCT. All analyses were performed on the intention-to-treat principal with all patients in their allocated arms. Adding to the prospective comparison of the efficacy between allo-HSCT and chemotherapy, we also retrospectively performed subgroup analysis by age. Statistical analyses were conducted using the SAS software package (SAS Institute, Inc, Cary, NC).

3 Results

3.1 Study patients and genetical allocation

Five hundred and three de novo AML patients aged from 15 to 50 years participated in the AML97 comparison of allo-HSCT with chemotherapy as a post-remission therapy. Of 392 patients achieved CR, 62 patients were excluded from the analysis because of insufficient data mainly deficient clinical data at diagnosis which were essential to verify their classification. Three hundred and thirty evaluable patients were classified into the good ($n = 149$), intermediate ($n = 162$) or poor risk ($n = 19$) groups using the scoring system described above (Fig. 1). The 5-year OS

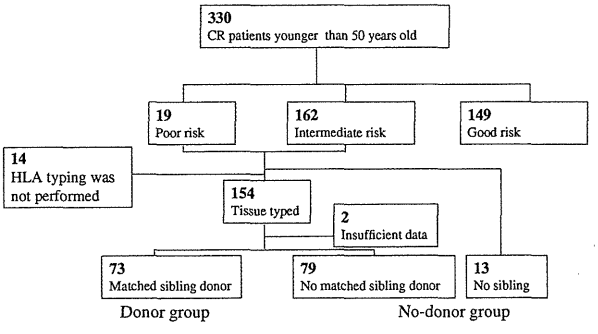

Fig. 1 Overview of patients included in analysis by risk classification, HLA typing, and donor availability

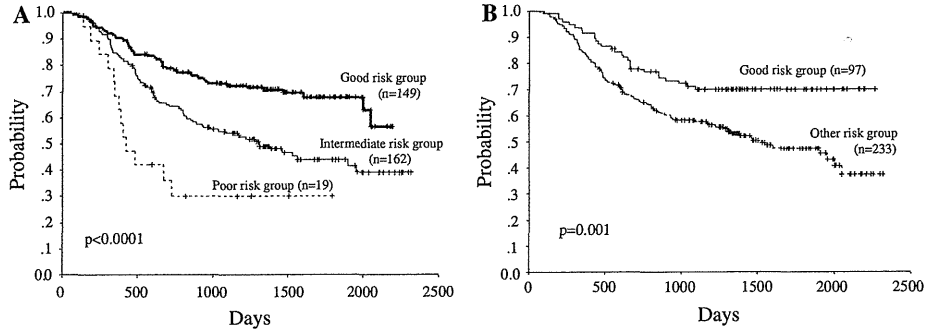

Fig. 2 Overall survival of patients in CR according to JALSG scoring system (**a**) and by cytogenetic studies (**b**)

rates of the CR patients with good, intermediate and poor risk were 68, 44 and 30%, respectively [hazard ratio (HR), 0.51 (good vs. intermediate) and 0.25 (good vs. poor), respectively; 95% confidential interval (CI), 0.35–0.73 (good vs. intermediate) and 0.14–0.48 (good vs. poor); $p < 0.0001$; Fig. 2a]. Among the intermediate and poor risk patients with living siblings, 154 patients and their siblings were examined for their HLA types. Seventy-three of these patients had an HLA-identical sibling and were assigned to the donor group. Thirteen patients with no siblings and 79 patients without an HLA-identical sibling were assigned to the no-donor group (92 patients). Finally, one patient in donor group and one patient in no-donor group were excluded from the analysis because of their insufficient data of survival (Fig. 1). The follow-up durations of the donor and no-donor groups were 1854 days (range 163–3176 days) and 1010 days (range 93–3008 days), respectively.

3.2 Patient characteristics of donor versus no-donor groups

Table 2 shows the characteristics of patients in the donor and no-donor groups. The distributions of these features were comparable in both groups with respect to age, gender, initial WBC count, MPO positivity of blasts, FAB subtype, performance status, prognostic risk according to JALSG score, presence of favorable cytogenetic abnormalities, and the groups of post-remission chemotherapy.

3.3 Donor group

Fifty-six patients (76%) in the donor group actually underwent allo-HSCT (Table 2). Thirty-eight patients (52%) received an allo-HSCT during CR1 at a median of 159 days (range 43–314 days) from CR1. Eighteen patients underwent allo-HSCT after relapse. The median times between CR1 and relapse and between CR1 and a transplantation were 183 days (range 39–757 days) and 248 days (range 157–973 days), respectively. Thirty and 24 patients were transplanted after undergoing a conditioning regimen with or without total body irradiation (TBI), respectively, and conditioning information was not available for 2 patients. The sources of transplanted stem cells were bone marrow cells ($n = 26$), peripheral blood cells ($n = 27$) and bone marrow cells together with peripheral blood cells ($n = 2$). Twenty-nine of the 56 patients in the donor group who underwent allo-HSCT remain alive. Twenty patients died of recurrent leukemia and 7 of transplant-related causes. Seventeen patients allocated to the donor group did not receive a transplantation for the following reasons; patients' refusal ($n = 6$), donors' refusal to donate ($n = 2$), physician's decision ($n = 1$), disease progression before transplantation ($n = 2$), donor health problems ($n = 2$) and unknown reasons ($n = 4$).

3.4 No-donor group

Of the 92 patients in the no-donor group, 42 eventually underwent HSCT (Table 2): autotransplantation ($n = 3$), allo-HSCT from HLA mismatched-related donors ($n = 4$), allo-HSCT from an HLA matched-unrelated donor ($n = 28$), and allo-HSCT from an HLA-mismatched unrelated donor ($n = 7$). Eleven patients underwent a transplantation during CR1 from an unrelated donor or mismatched-related donor at a median of 281 days (range 170–1700 days) from CR1, significantly later than those transplanted during CR1 in the donor group ($p < 0.001$). Thirty-one patients received a transplantation after relapse. The median times between CR1 and relapse and between CR1 and a transplantation were 329 days (range 92–876 days) and 519 days (range 167–1373 days), respectively.

3.5 Comparison of donor versus no-donor groups

The actual risk of relapse at 8 years was significantly lower in the donor group than in the no-donor group (52 vs. 77%, respectively, HR, 0.58; 95% CI, 0.39–0.88; $p = 0.008$; Table 3). The TRM did not significantly differ between the donor and the no-donor groups (16 vs. 17%, respectively, HR, 0.97; 95% CI, 0.34–2.80; $P = 0.959$; Table 3). Seven